

**NASA TECHNICAL  
MEMORANDUM**

NASA TM X-64546

**PHOTOGRAMMETRIC TECHNIQUES APPLICABLE  
TO EARTH RESOURCES ANALYSES**

By Paul A. Larsen  
Aero-Astroynamics Laboratory

August 21, 1970

**CASE FILE  
COPY**

**NASA**

*George C. Marshall Space Flight Center  
Marshall Space Flight Center, Alabama*

TECHNICAL REPORT STANDARD TITLE PAGE

1. Report No. TM X-64546	2. Government Accession No.	3. Recipient's Catalog No.	
4. Title and Subtitle PHOTOGRAMMETRIC TECHNIQUES APPLICABLE TO EARTH RESOURCES ANALYSES		5. Report Date August 21, 1970	
		6. Performing Organization Code	
7. Author(s) Paul A. Larsen		8. Performing Organization Report No.	
9. Performing Organization Name and Address Aero-Astroynamics Laboratory George C. Marshall Space Flight Center Marshall Space Flight Center, Alabama 35812		10. Work Unit No.	
		11. Contract or Grant No.	
12. Sponsoring Agency Name and Address		13. Type of Report and Period Covered  TECHNICAL MEMORANDUM	
		14. Sponsoring Agency Code	
15. Supplementary Notes This work performed in Aerospace Environment Division, Aero-Astroynamics Laboratory, Science and Engineering Directorate			
16. Abstract  The uses of photogrammetry as a tool for studying our natural resources and as an aid in understanding and defining environmental problems confronting the inhabitants of earth are discussed. Numerous applications of photogrammetry from the past are cited, and several very recent applications are discussed briefly, the intent being to help researchers and engineers in related fields see photogrammetry as an aid in their endeavors. Actual measurements of physical features of the earth's and moon's surfaces, which were made photogrammetrically on stereograms prepared from Apollo 6 and Apollo 8 vertical orbital photographs, are shown. The Skylab Experiment S-190, "Six Camera Multispectral Photography," is discussed, and a graphical analysis dealing with the percentage of ground observable by the Skylab cameras as a function of cumulus cloud coverage is presented. The science of photogrammetry has proved to be an exceedingly useful and practical tool in the past, and all indications are that its applicability to life's current and future problems and tasks is just being discovered.			
17. Key Words Photogrammetry      Meteorology Aerial Photography      Earth Geography      Resources Geology		18. Distribution Statement PUBLIC RELEASE: <i>Wm E. D. Geissler</i> E. D. Geissler Director, Aero-Astroynamics Lab.	
19. Security Classif. (of this report) UNCLASSIFIED	20. Security Classif. (of this page) UNCLASSIFIED	21. No. of Pages 60	22. Price



# TABLE OF CONTENTS

	<u>Page</u>
I. INTRODUCTION.....	1
II. PHOTOGRAMMETRIC APPLICATIONS.....	3
A. Activities Associated with Earth Resources to Which Photogrammetric Techniques are Applicable.....	3
B. Activities Associated with Earth Problems to Which Photogrammetric Techniques are Applicable.....	5
III. PHOTOGRAMMETRIC MEASUREMENTS AND PHOTOGRAPHIC INTERPRE- TATIONS RELATED TO EARTH RESOURCES.....	7
A. Photogrammetric Measurements from Aerial Photographs of the Fort Sill, Oklahoma Area.....	8
B. Earth Resources, Observations, Photogrammetric Measurements, and Topographic Information from Apollo 6 Photographs 1443, 1444, and 1445.....	13
C. Earth Resources Observations and Photogrammetric Measurements from Apollo 6 Photographs 1451 and 1452.	30
D. Photogrammetric Measurements and Photographic Inter- pretations from Apollo 8 Lunar Orbital Photographs 2066 and 2067.....	36
IV. SKYLAB EXPERIMENT S-190: "SIX CAMERA MULTISPECTRAL PHOTOGRAPHY".....	40
V. ANALYSIS OF GROUND OBSERVABLE BY SKYLAB CAMERA THROUGH CUMULUS CLOUD COVERAGE.....	41
VI. SEVERAL RECENT PHOTOGRAMMETRIC APPLICATIONS BY UNIVERSI- TIES, COMPANIES, AND OTHER GOVERNMENT AGENCIES.....	45
A. Side-Looking Airborne Radar (SLAR) as a Geophysical Tool.....	45
B. Thermal Pollution Revealed by Infrared Radiation.....	47
C. Automatic Stereoplotting for Mapping and Measuring Polluted Air Masses.....	51
D. "Space Age" Road Map Which Resulted from Gemini V Mission.....	54
VII. SUMMARY REMARKS.....	54

# LIST OF TABLES

<u>Table</u>	<u>Title</u>	<u>Page</u>
I	Parallax Measurements from Figure 2.....	8
II	Results of Photogrammetric Measurements Made on Figure 2.....	13
III	Photogrammetric Parameters of Apollo 6 Photographs 1443, 1444, and 1445.....	14
IV	Results of Photogrammetric Measurements Made on Figure 6.....	29
V	Results of Photogrammetric Measurements Made on Figure 9.....	36
VI	Geographical Coordinates of Principal Points of Apollo 8 Photographs 2066 and 2067.....	36

# LIST OF ILLUSTRATIONS

<u>Figure</u>	<u>Title</u>	<u>Page</u>
1	Aerial Photograph of Fort Sill, Oklahoma Area.....	9
2	Stereogram of Fort Sill, Oklahoma Area.....	11
3	Apollo 6 Orbital Photograph 1443.....	16
4	Apollo 6 Orbital Photograph 1444.....	17
5	Apollo 6 Orbital Photograph 1445.....	19
6	Stereogram of Apollo 6 Orbital Photographs 1444 and 1445.....	22
7	Stereogram of Apollo 6 Orbital Photographs 1443 and 1444.....	23
8	Topographic Information Inferred from Apollo 6 Photographs 1443, 1444, and 1445.....	25
9	Stereogram of Apollo 6 Orbital Photographs 1451 and 1452.....	31
10	Apollo 6 Orbital Photograph 1451.....	33
11	Stereogram of Apollo 8 Lunar Orbital Photographs 2066 and 2067.....	37
12	Apollo 8 Lunar Orbital Photograph 2066.....	38
13	Location of Skylab Experiment S-190.....	42
14	Ground Observable by Skylab Camera Through 32.5 Percent Cumulus Cloud Coverage.....	43
15	Ground Observable by Skylab Camera Through 32.5 Percent Cumulus Cloud Cover, Versus Sun Angle.....	46
16	Ground Observable by Skylab Camera, as a Function of Cumulus Cloud Coverage, Assuming a 20° Sun Elevation...	47
17	Radar Mosaic of Darien Province, Panama, and Northwest Colombia, South America.....	48

# LIST OF ILLUSTRATIONS (Continued)

<u>Figure</u>	<u>Title</u>	<u>Page</u>
18	Thermal Pollution in the Connecticut River Revealed by Infrared Radiation.....	50
19	Color Stereogram Showing Air Pollution in the Port Townsend, Washington Area.....	52
20	Topographic Map of Air Pollution in the Port Townsend, Washington Area.....	53
21	Gemini Photomap of the Tucson, Arizona Vicinity.....	55

## DEFINITION OF SYMBOLS

<u>Symbol</u>	<u>Definition</u>
H'	average height of the spacecraft or aircraft above the terrain photographed
b	the photographic base, or average distance between principal point and conjugate (corresponding) principal point, on the two photographs of a stereogram
$\Delta p$	the difference in parallax measurements between two points on a stereogram
$\Delta h$	the difference in elevation between two points observable on a stereogram
D	linear distance between objects on a photograph
M.R.	metric reading from stereoscope, when measuring horizontal distances
1/S	scale of photography

### Specialized Terms

Alluvial Fan	an alluvial fan is a gently sloping conical structure formed by deposits from a stream emerging from a steep, narrow valley, onto a broader lowland
Dendritic Drainage Pattern	a dendritic drainage pattern is formed where the underlying rock structure offers uniform resistance, and tributaries subdivide headward like the limbs of a tree
Intrusive Masses	masses of Plutonic Igneous Rock formed by consolidation of magma beneath the surface
Mesa	a flat-topped rocky hill with steeply sloping sides, common in southwestern United States
Perlite	volcanic glass with a concentric shelly structure
Playa	a temporary lake, formed by sporadic rain, which evaporates during the dry season, leaving a sunbaked floor of clay, silt, and salt
SLAR	<u>S</u> ide <u>L</u> ooking <u>A</u> irborne <u>R</u> adar

## TECHNICAL MEMORANDUM X-64546

### PHOTOGRAMMETRIC TECHNIQUES APPLICABLE TO EARTH RESOURCES ANALYSES

#### SUMMARY

Applications of photogrammetry to studies of earth resources and earth problems, including the earth environment, are listed. Photogrammetric measuring techniques are used to obtain elevation differences between various points visible on stereograms constructed from Apollo 6 and Apollo 8 earth orbital and lunar orbital photographs. Topographic information inferred from stereograms prepared from orbital photographs of southwest New Mexico is presented, along with photographic interpretations. Skylab Experiment S-190, "Six Camera Multispectral Photography," is discussed, and a graphical analysis showing the percentage of ground observable by the Skylab cameras through various percentages of cumulus cloud coverages is reported. Several recent photogrammetric projects completed by universities, private industry, and government agencies are discussed briefly. Pertinent stereograms, a radar image, and an image prepared by infrared line-scanning techniques are shown, along with relevant photographic interpretations.

#### I. INTRODUCTION

As more and more emphasis is being placed on efficient utilization of the earth's limited resources, and as we become more aware of the deteriorating conditions of the earth's water and air, it becomes apparent that positive steps must be taken to (1) tap new areas of resource potential, and to make use of them in a conservative way to the best advantage of earth's future inhabitants, and (2) initiate such corrective measures as may be necessary to maintain the air in a breathable condition, and to keep the available supplies of water suitable for human consumption and the sustenance of other forms of plant and animal life on earth.

All human beings on earth will have to do their part to keep the earth suitable for sustaining lives of future generations. Scientists and engineers will, of necessity, play a large role in helping to solve the problems we face as inhabitants of earth. As in most professions, certain tools are employed to solve the problems encountered by the professionals. One very interesting and practical tool available to the engineer is the branch of science called "Photogrammetry." Photogrammetry is defined as the science or art of obtaining reliable measurements by means of photography.

It is the purpose of this paper (1) to show how the science of photogrammetry can be employed in the study of earth resources, (2) to describe how it can be helpful in understanding and defining some of the problems of water and air pollution, and (3) to mention a large number of typical applications of photogrammetry so that these listings may suggest or imply to potential users applications to many other problems.

To try to advance these goals, the author has surveyed a large number of professional papers in the photogrammetry field, pertinent textbooks, and sales literature of corporations engaged in the business of photogrammetric services, and has listed photogrammetric applications pertinent to earth resources and earth problems, including environment and atmosphere. In addition, use has been made of orbital photography from the Apollo 6, Apollo 8, and Gemini V missions to demonstrate actual basic photogrammetric measuring techniques and photo-interpretation methods of potential use to persons needing quantitative information from photographs, but whose parent organizations are not equipped with some of the more exotic and precise photogrammetric equipment which is commercially available today.

After attending the 1970 ACSM-ASP Convention (American Congress on Surveying and Mapping - American Society of Photogrammetry), the author selected several fairly recent applications of photogrammetric engineering which were displayed and/or discussed at the convention. Four of these applications, which reflect some of the current photogrammetric activities being conducted by government agencies, universities, and private industry, are discussed.

Skylab Experiment S-190, "Six Camera Multispectral Photography," is described, and a graphical analysis showing the percentage of ground observable by the Skylab cameras through various percentages of cumulus cloud coverages is included.

The author wishes to express his sincere appreciation to his many colleagues in government agencies, private industry, and universities, who were so very helpful in furnishing suggestions, comments, photographic samples, technical reports, and brochures, all contributing in various ways to the completion of this report.

Special thanks are extended to Major John S. Thorsen of the U. S. Army Engineer Topographic Laboratories; Miss Theresa M. Sousa of the United States Geological Survey, Department of the Interior; Mr. Douglas Esten and Mr. George Loelkes of Raytheon-Autometric; Dr. S. A. Veress of the University of Washington; Mr. Curt Rottweiler of Bendix-Aerospace; Mr. Robert Hill of NASA-Manned Spacecraft Center; Dr. Dean C. Merchant of Ohio State University; and Mrs. Evelyn Carter, Mrs. Sarah Hightower, Mrs. Irene Dolin, Mr. S. Clark Brown and Mr. Richard Tinus of NASA-Marshall Space Flight Center.

## II. PHOTOGRAMMETRIC APPLICATIONS

It would be extremely difficult for a person engaged in any particular field of science or engineering to be even reasonably familiar with all the types of programs, projects and activities that are currently going on in that field, which have been attempted or completed in the past or which are being considered for future emphasis. Accordingly the following lists of activities to which photogrammetric techniques are applicable are by no means intended to be all-inclusive. They are, however, the results of a diligent search in sources such as technical papers, textbooks, literature from private firms engaged in the sale of photogrammetric services, and Photogrammetric Engineering, the Journal of the American Society of Photogrammetry. The application lists are divided into two categories: (1) Activities associated with Earth Resources to Which Photogrammetric Techniques are Applicable, and (2) Activities Associated with Earth Problems to Which Photogrammetric Techniques are Applicable.

### A. Activities Associated with Earth Resources to Which Photogrammetric Techniques are Applicable

1. Rural and urban land use capability studies.
2. Soil classification and moisture content analyses.
3. Geological resource surveys to locate mineral deposits, oil provinces, and fossil fuel.
4. Determination of snow depths, using suitable ground control devices such as snow depth markers.
5. Land classification studies.
6. Vegetation type and condition surveys.
7. Stockpile inventories.
8. Land area development and exploitation.
9. Mapping of geological phenomena to identify faults, folds, and intrusive masses.
10. Agricultural studies.



11. Real estate development.
12. Strip mining operations.
13. Rangeland condition determinations.
14. Preparation of space photomaps (1:250,000 scale), which combine medium scale line maps with space imagery.
15. Power plant site selection planning and development.
16. Soil conservation and classification studies.
17. Recreational area planning.
18. Lumber (forestry) production studies.
19. Definition of economical location of highway construction.
20. Tectonic map preparation.
21. Preparation of photo-mosaics of various parts of countries.
22. Industrial expansion planning.
23. Zoological applications such as identification and inventorying of animal species.
24. Landform analyses.
25. Preparation of precise planimetric maps (near-orthographic), resulting from orbital photographs of proper design.
26. Differentiation between healthy deciduous and evergreen trees, using infrared sensitive color film.
27. Terrain mapping in locations obscured by cloud cover, using side-looking airborne radar.
28. Geophysical studies.
29. Cloud cover analyses.
30. Industrial site selection, planning, and development.
31. Classification of ground cover types.
32. Studies of tropical and sub-tropical landforms and vegetation.

33. Soil moisture characteristic determinations.
34. Estuary and coastal studies.
35. Aquacultural applications such as fish school location determinations.
36. Studies of water masses and current flow.
37. Groundwater condition determinations.
38. Shoal identification.
39. Biological activity surveys, such as identification of Plankton concentrations of fish schools.
40. Land drainage studies such as drainage pattern and watershed characteristic analyses.
41. Waterway, river, canal, and harbor development.
42. Surveys for locating and mapping ground water resources.
43. Mapping of global sea state and surface temperature to help weather forecasters, and the shipping and fishing industries.
44. Water resources development.
45. Coastal hydrography and bathymetry surveys.

B. Activities Associated with Earth Problems  
to Which Photogrammetric Techniques are Applicable

1. Determining locations of air and water pollution sources.
2. Smog determination.
3. Air pollution analyses.
4. Monitoring of gaseous wastes.
5. Geological determination of likelihood of landslides occurring in populated areas.
6. Forest disease and forest fire surveys.

7. Construction site analyses to determine landslide potential, fault, and fracture zones.
8. Industrial waste disposal.
9. Transportation flow and automobile traffic evaluation studies.
10. Early detection of disease and/or pest infestation in crops or ground over, using infrared sensitive color film.
11. Sewer system planning and design.
12. Preparation of surveys for census estimating and urban planning.
13. Survey studies of dynamic features such as growth or decay of cities.
14. Urban area analyses.
15. Levee preparation analyses.
16. Irrigation planning studies.
17. Flood control studies.
18. Flood mapping.
19. Water pollution studies such as thermal, sewage, and industrial discharge analyses.
20. Studies of coastal deltas to determine channel filling, erosion, and flooding.
21. Surveys to monitor water quality.
22. Tracking and observation of erosion and sedimentation materials in bodies of water.
23. Studies of waves, swells, and slicks on water surfaces.
24. Fresh water and marine ecology.
25. Monitoring of water pollutants such as sewage and waste disposal and industrial discharges.
26. Biological activity analyses, such as identification of effluents.

27. Oil slick and oil spill detection, tracking, size determination, and mapping.
28. Studies of sediment concentration in water.
29. Medical applications such as human bone deformation and fracture studies, using X-ray stereoscopy.
30. Dental applications such as tooth, jawbone, and bite analyses, using X-ray stereoscopy.

### III. PHOTOGRAMMETRIC MEASUREMENTS AND PHOTOGRAPHIC INTERPRETATIONS RELATED TO EARTH RESOURCES

This section of the report demonstrates the value of vertical aerial or orbital photographs when one desires (1) to measure differences in elevation between two points which are imaged on both members of a stereographic pair of vertical photographs, and (2) to interpret various types of engineering and scientific information contained within vertical photographs.

The optical instrument used for measuring the absolute parallax\* of the points selected on the enclosed stereograms, was the Abrams CB-1 Lens Stereoscope, equipped with a Height Finder Model HF-2 Parallax Bar. Both pieces of equipment are manufactured by the Abrams Instrument Corporation of Lansing, Michigan.

Photographs used for constructing the stereograms on which measurements were made consisted of aerial photographs taken near Fort Sill, Oklahoma, by the Army Map Service, Apollo 6 Orbital Photographs of southwestern New Mexico, and Apollo 8 lunar photographs of an area on the lunar farside, west of craters Korolev, Krylov, and Doppler. The original photographs (9" x 9" aerial and orbital) were reduced in size using a Polaroid MP-3 Multi-Purpose View camera to facilitate making measurements on the stereograms with the CB-1 Lens Stereoscope and HF-2 Parallax Bar.

The format followed in this section consists generally of showing an enlarged photograph of the area under consideration, with the various measurement points labelled, and then including a photograph of the

---

\* A discussion of parallax, preparation of stereograms, and the related geometry which enables one to measure differences in elevation from photographs can be found in reference 1.

stereogram on which the parallax measurements were actually made. For the Apollo 6 and Apollo 8 photography, an interpretation of each stereogram is included, and for one of the Apollo 6 stereograms, a hand-sketched form line topographic plot of the area photographed is included to illustrate the usefulness of stereograms in preparing such a plot.

#### A. Photogrammetric Measurements from Aerial Photographs of the Fort Sill, Oklahoma Area

Figure 1 is a larger scale photograph of the left-hand member of the stereogram of the Fort Sill, Oklahoma area shown in figure 2. On figure 1 are marked several points, with letter designations. Point B is a point on the north shore of a small reservoir; point A is on a small mountain peak approximately 800 meters northeast of point B; and point C is a point on top of Mount Sherman, about 1300 meters northeast of point A. Point D, at the location of Fort Sill's West Gate on McKenzie Hill Road is approximately 2150 meters south-southeast of point B. The determination of the differences in elevations between points A and B, B and C, and C and D, using photogrammetric measuring techniques is described in the following paragraphs. Some mathematical detail is given in this first example to illustrate the techniques used. Subsequent measurement examples, using this and other stereograms, will include only the main steps and results, since the techniques used are the same as those used in the first example.

For the aerial photographs which figure 2 comprises, the average flying height  $H'$  above the datum (the datum being the average terrain elevation) was 26,100 feet. The average photographic base  $b$  (distance between the principal point and the conjugate principal point) measured on the stereogram is 36.25 mm.

Table I gives the values of absolute parallax measured for points A and B using the lens stereoscope and parallax bar (five measurements for each point), the differential parallax  $\Delta p$ , and the average of  $\Delta p$ .

Table I. Parallax Measurements from Figure 2

A	4.88	4.88	4.90	4.91	4.91
B	4.15	4.14	4.17	4.19	4.18
$\Delta p$	.73	.74	.73	.72	.73
$\Delta p_{avg} = .73 \text{ mm}$					

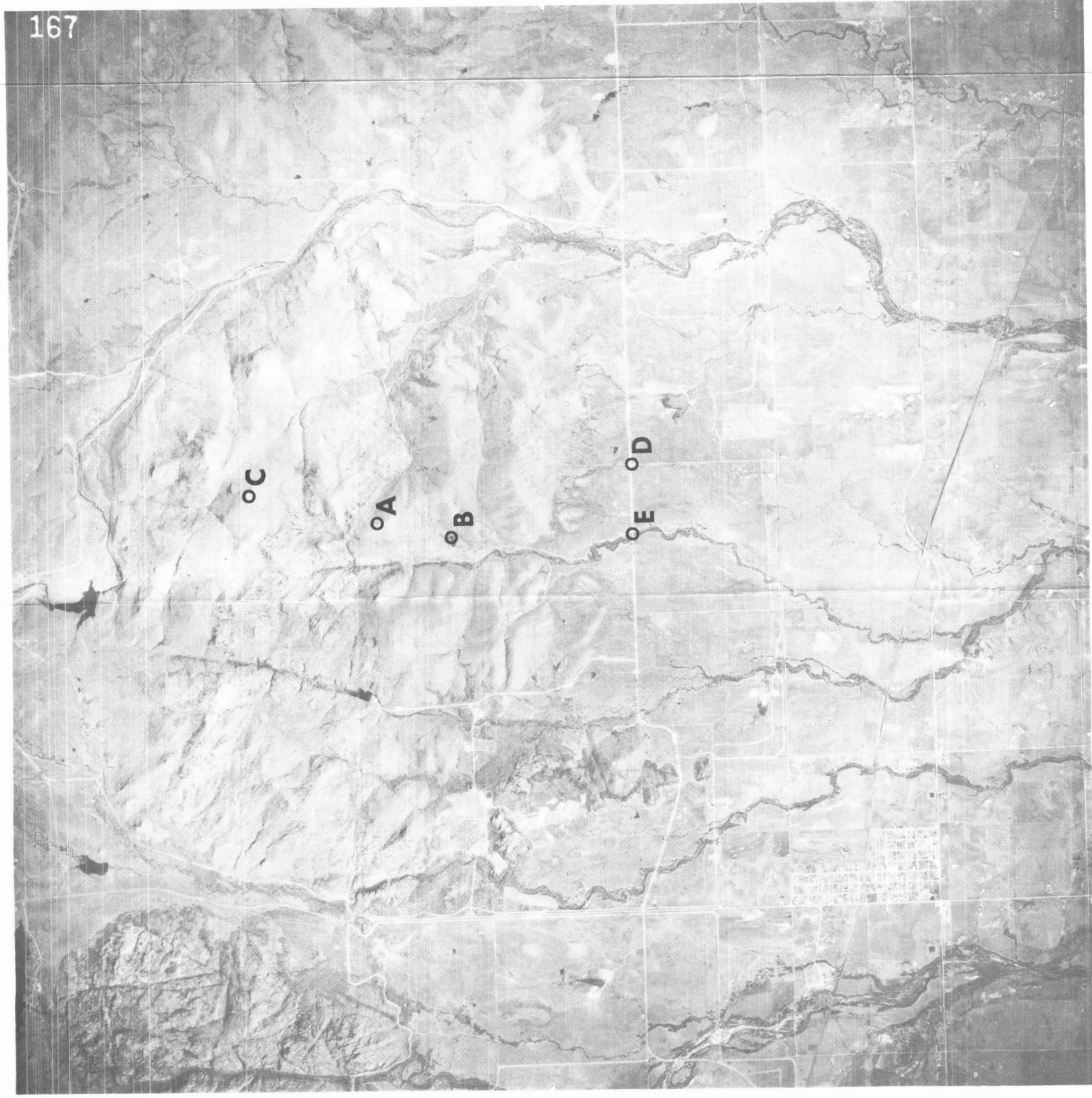
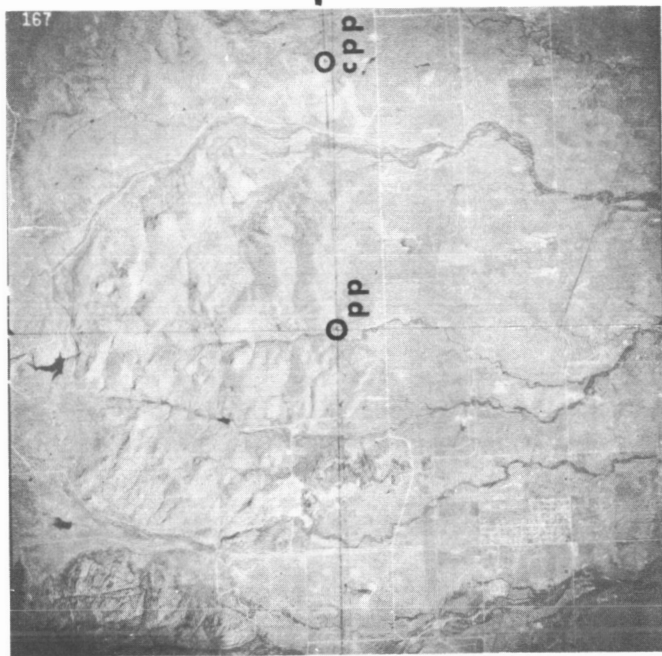
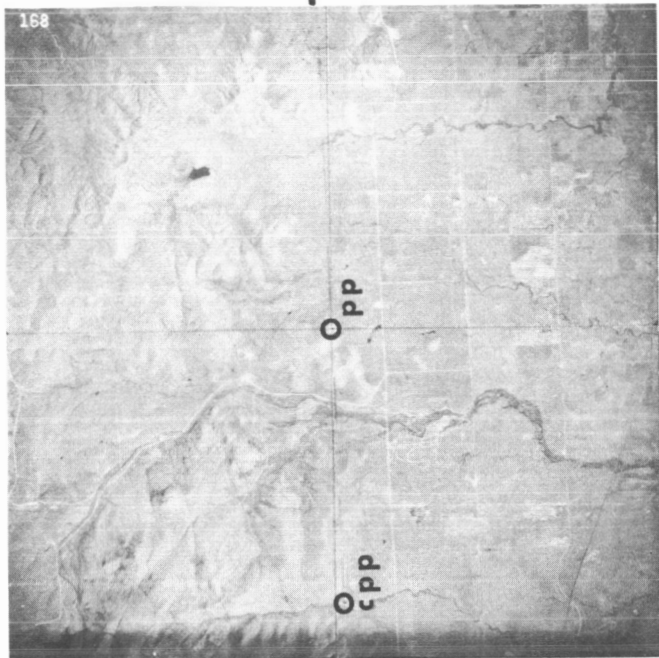


FIG. 1. AERIAL PHOTOGRAPH OF FORT SILL, OKLAHOMA AREA

Flight  
Line



pp = Principal Point

cpp = Conjugate Principal Point

FIG. 2. STEREOGRAM OF FORT SILL, OKLAHOMA AREA

The equation

$$\Delta h = \frac{H' \Delta p}{b}$$

is used to calculate the difference in elevation between the points. Therefore, substituting the preceding values into this equation yields

$$\Delta h_{A-B} = \frac{H' \Delta p}{b} = \frac{26,100 \text{ ft} \times .73 \text{ mm}}{36.25 \text{ mm}} = 526 \text{ ft.}$$

To check this answer, reference was made to Army Map Service (A.M.S.) Sheet 6253 II of Cache, Oklahoma, dated June 1965 [2]. This map showed  $\Delta h_{A-B}$  to be 559 feet. Therefore, calculating the percent error between actual elevations and the photogrammetric measurement demonstrated herein, we obtain

$$\text{Percent Error} = \frac{559 - 526}{559} \times 100 = 5.91.$$

When measuring parallax to determine the difference in elevation between point B (North Shore of Reservoir), and point C (peak of Mount Sherman), the average of seven measurements on each point yielded a  $\Delta p_{B-C}$  of 1.097 mm. A  $\Delta h_{B-C}$  of 790 feet resulted from substituting this value in the equation. Referring to AMS Sheet 6253 II, we obtain a  $\Delta h_{B-C}$  of 827 feet. The resulting error between actual elevation and photogrammetric measurement was 4.48 percent.

When measuring parallax to determine the difference in elevation between point C (peak of Mount Sherman) and point D (West Gate of Fort Sill on McKenzie Hill Road), the average of seven parallax measurements on each point yielded a  $\Delta p_{C-D}$  of 1.258 mm. A  $\Delta h_{C-D}$  of 909 feet resulted from substituting this value in the equation. Referring to AMS Sheet 6253 II, a  $\Delta h_{C-D}$  of 906 feet was obtained. The resulting percent error between actual elevation and photogrammetric measurement is .331. Table II summarizes the results of the photogrammetric measurements made from the stereogram of the Fort Sill, Oklahoma area shown in figure 2.



Table II. Results of Photogrammetric Measurements Made on Figure 2

Two Points Considered	$\Delta h$ (ft) Determined Photogrammetrically	$\Delta h$ (ft) Determined from AMS Map	Percent Error
A,B	526	559	5.91
B,C	790	827	4.48
C,D	909	906	0.331

The Abrams CB-1 Lens Stereoscope can also be utilized to directly measure linear distances on vertical photographs. For example, to measure the linear distance between points D (West Gate of Fort Sill on McKenzie Hill Road) and point E (the center of a bridge crossing the gully just west of point D) shown on figure 1, the procedure is as follows. The index line and cylinder gauge of the HF-2 parallax bar are both set at zero. The movable index dot is placed on the point D, then the cylinder gauge is turned until the movable index dot rests over point E. This was done between points D and E, and a reading of 5.98 mm was obtained from the parallax bar. This value is then substituted into the equation:

$$D = \frac{M.R. \times .0394}{1/S},$$

where M.R. is the parallax bar reading (5.98 mm in this case), .0394 is a constant, and  $1/S$  is the photographic scale in feet. Substituting  $M.R. = 5.98$  mm and the photographic scale  $S$  of  $1''/11,000$  feet into the equation, the resultant linear distance "D" between points D and E is 2580 feet. A measurement of this same distance on the map yielded 2610 feet. The percent error, then, is 1.15.

B. Earth Resources, Observations, Photogrammetric Measurements,  
and Topographic Information from Apollo 6  
Photographs 1443, 1444, and 1445

Three Apollo 6 photographs, 1443, 1444, and 1445, which covered a portion of the area between Las Cruces, New Mexico, and Tucson, Arizona, were examined closely, for two reasons. First, it appeared worthwhile to illustrate the usefulness of the earth orbital photography for

applications related to earth resource analyses, in conjunction with the forthcoming Skylab program; and secondly, when preparing stereographic pairs of vertical orbital or aerial photographs for topographical and photogrammetric analyses, it has been found quite helpful to have a good mental picture or synoptic view of the entire area of terrain being interpreted.

The areas which are visible in Apollo 6 photograph frames 1443, 1444, and 1445, shown as figures 3, 4, and 5, are located in the "Basin and Range Province." This province includes a portion of west Texas, southwestern New Mexico, southern Arizona, southeastern California, western Utah, and almost all of Nevada. The "Basin and Range Province" consists of isolated mountain ranges separated by wide desert plains, many lakes, ancient lake beds, and alluvial fans. Accordingly, the three photographs mentioned above were interpreted from two aspects: (1) to see what topographic knowledge of the area could be gleaned by observation and inference, and (2) to actually define some dimensions of the topographical features in the area by making certain typical photogrammetric measurements of prominent physical features revealed in the photographs.

The three photographs were essentially "vertical," i.e., sufficiently vertical to permit photogrammetric measurements with a lens stereoscope equipped with a parallax bar. Various photogrammetric parameters of the three photographs are shown in Table III.

Table III. Photogrammetric Parameters  
of Apollo 6 Photographs 1443, 1444, and 1445

PARAMETER	PHOTOGRAPH		
	1443	1444	1445
Geographic Coordinates:			
Latitude	31°58' 03.099"	32°02' 45.840"	32°05' 52.683"
Longitude	-109°39' 41.360"	-108°59' 59.528"	-108°20' 14.688"
Altitude	704,872.5 ft.	703,899.0 ft.	701,597.7 ft.
Rotation Angles:			
X-Tilt	0°39' 35.599"	0°35' 04.026"	-0°01' 17.405"
Y-Tilt	-1°15' 21.739"	-0°51' 47.485"	-0°34' 49.499"
Heading	81°11' 07.484"	81°34' 10.152"	81°57' 42.848"

PAGE 15 INTENTIONALLY  
LEFT BLANK

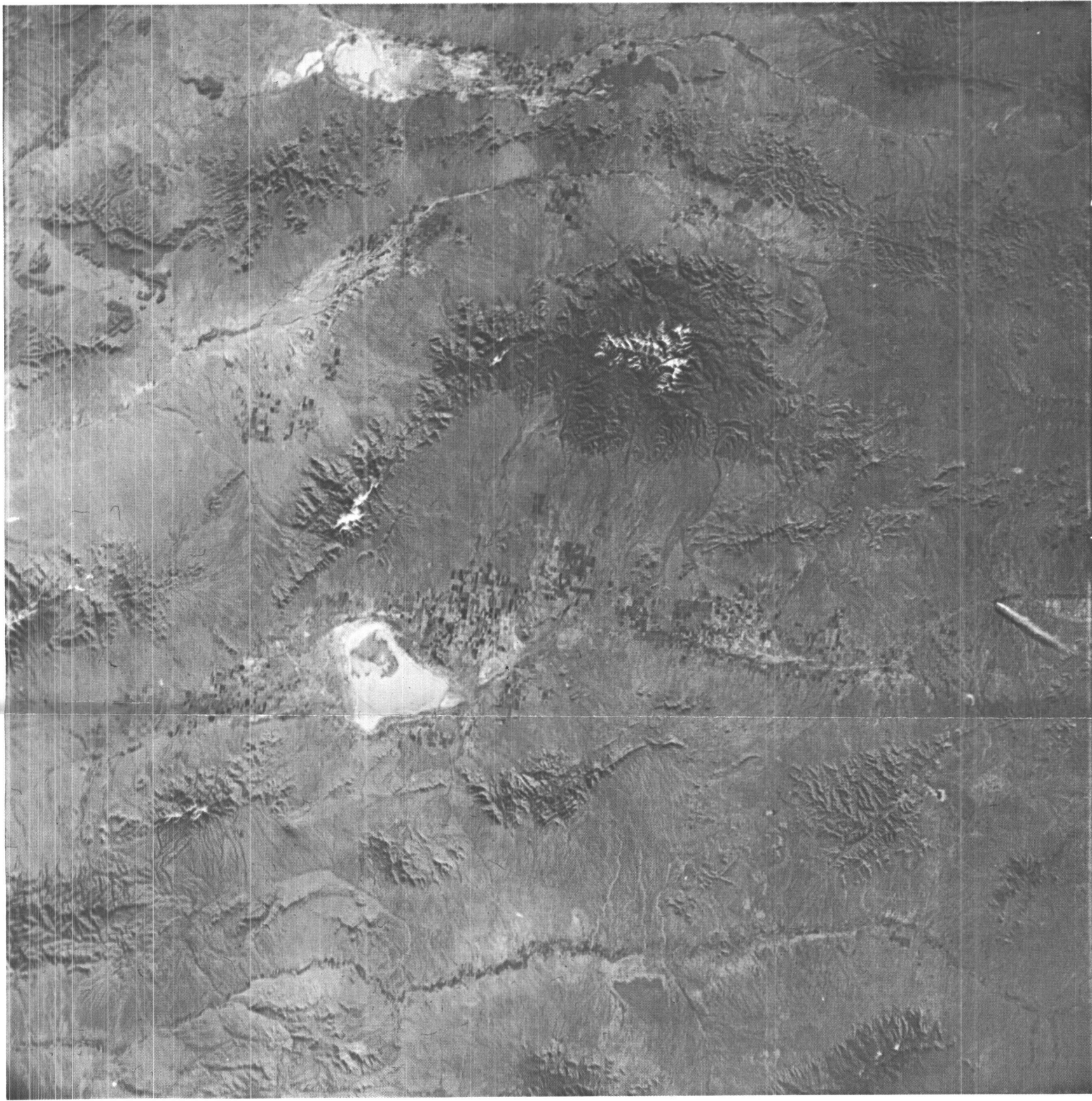


**FIG. 3. APOLLO 6 ORBITAL PHOTOGRAPH 1443**



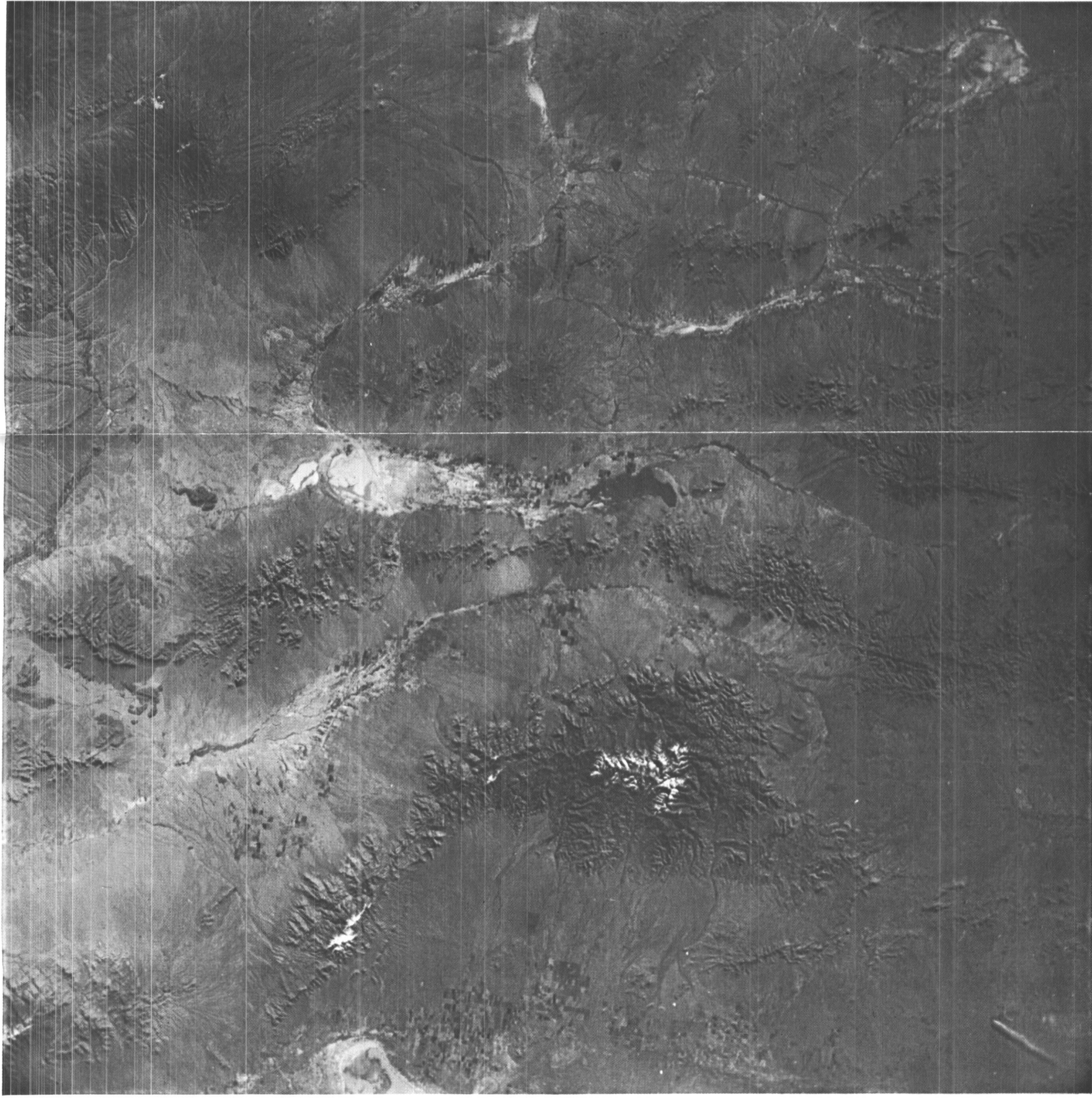


**FIG. 4. APOLLO 6 ORBITAL PHOTOGRAPH 1444**

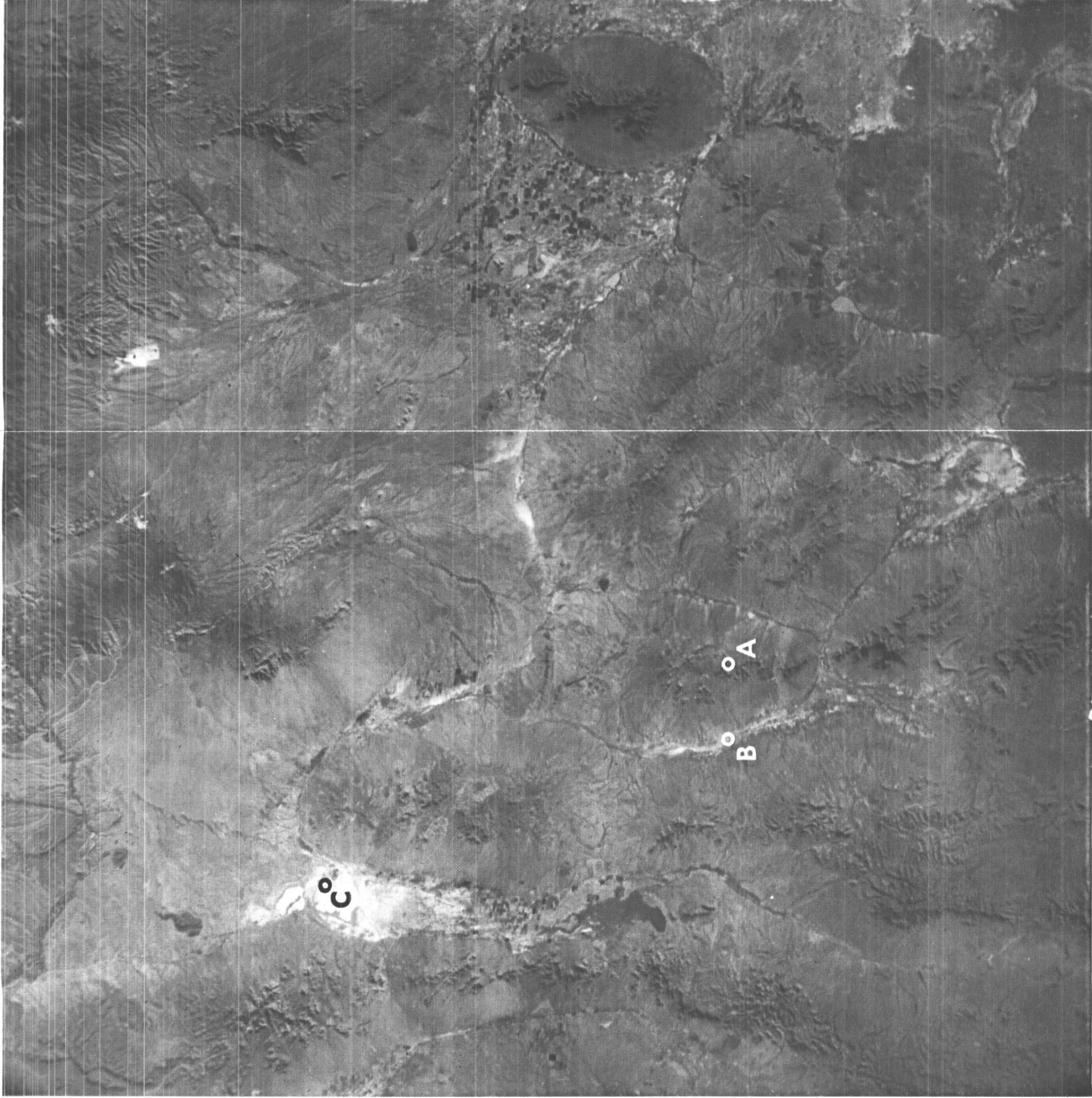


FIG. 5. APOLLO 6  
ORBITAL  
PHOTOGRAPH  
1445



As a first step, photographs 1444 and 1445 were viewed singly, (figures 4 and 5) and as a stereographic pair (figure 6). Photographs 1443 and 1444 were also viewed singly (figures 3 and 4) and as a stereographic pair (figure 7). From these observations, a topographic map of the area was hand-sketched, as shown in figure 8. Mountains, rivers, playas, highways, lakes, and areas in cultivation were readily discernible on the photographs. These geographic features were then indicated on the sketch. Other points of interest which were interpreted from the photographs were an airport southwest of Hurley, New Mexico (photograph 1445, shown in figure 5), and a smoke cloud, evidently emanating from an industrial plant smokestack or perhaps from one of the copper smelter chimneys, on White Water Draw, east of Potter Mountain, in Arizona (photograph 1443, shown in figure 3). An interesting fact resulting from the observation of this smoke cloud is that the cloud prevents the terrain beneath it from being photographed by a conventional camera using standard black and white film. Likewise, the shadow of the cloud, for all practical purposes, prevents photographic viewing of another portion of the terrain, almost as large as the projected area of the cloud itself at the condition of sun elevation which existed when these photographs were taken. The reader is referred to section V for further discussion and a geometric analysis of an associated phenomenon, that of cumulus clouds and their effects on the Skylab camera's ability to photograph earth's terrain at various percentages of cumulus cloud coverage, and at various sun elevations. "It is known that large smoke plumes from heavy industries can be viewed from space, and if they are viewed repetitively, significant information would be derived for helping to understand the dynamics of air movement in the particular area under study. It has been pointed out that studies of the fate and effects of air pollutants such as this are urgently needed" (quoted from reference 3).

It is pointed out here that even though cameras loaded with standard panchromatic film cannot penetrate haze from clouds or smoke, multispectral television cameras imaging in the 475 - 575 millimicron spectral band (blue-green) can provide acceptable haze penetration, and in addition, can provide maximum penetration of ocean, bay, and lake water to permit mapping of underwater features [3]. The first Earth Resources Technology Satellite (ERTS) will contain three moderate resolution multispectral television cameras such as the one described in reference 3, and will image three spectral bands simultaneously, 475 - 575 millimicrons (blue-green), 690 - 830 millimicrons (infrared), and 580 - 680 millimicrons (red). These three bands are used for (1) penetration of haze, ocean, bay and lake water; (2) maximum obscuration by water to permit precise shoreline mapping and estimates of relative moisture distribution and vegetation vigor on the ground; and (3) for discrimination of vegetation communities, recognition and identification of agricultural crops, and distribution of cultural features, respectively [4].

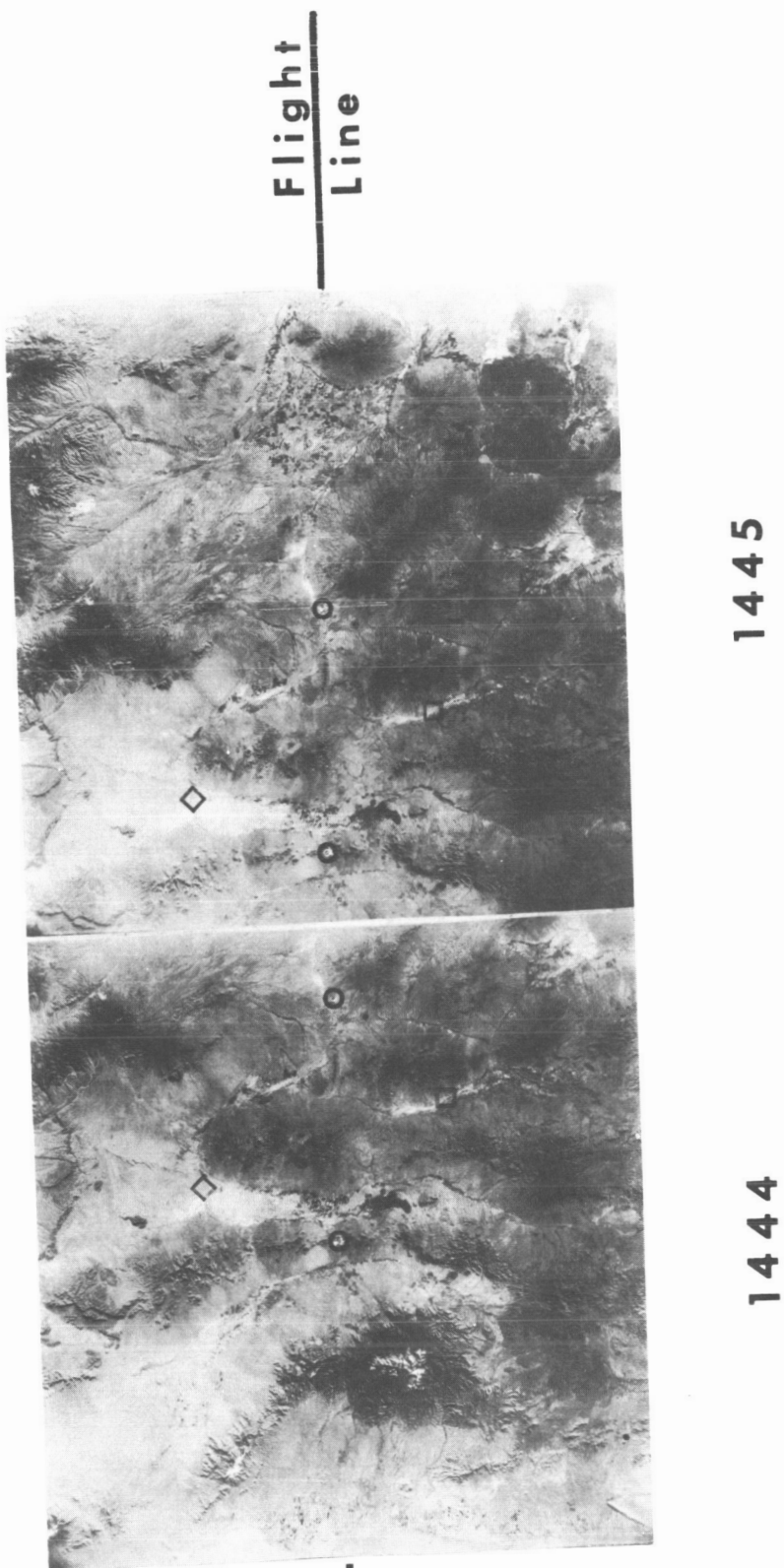
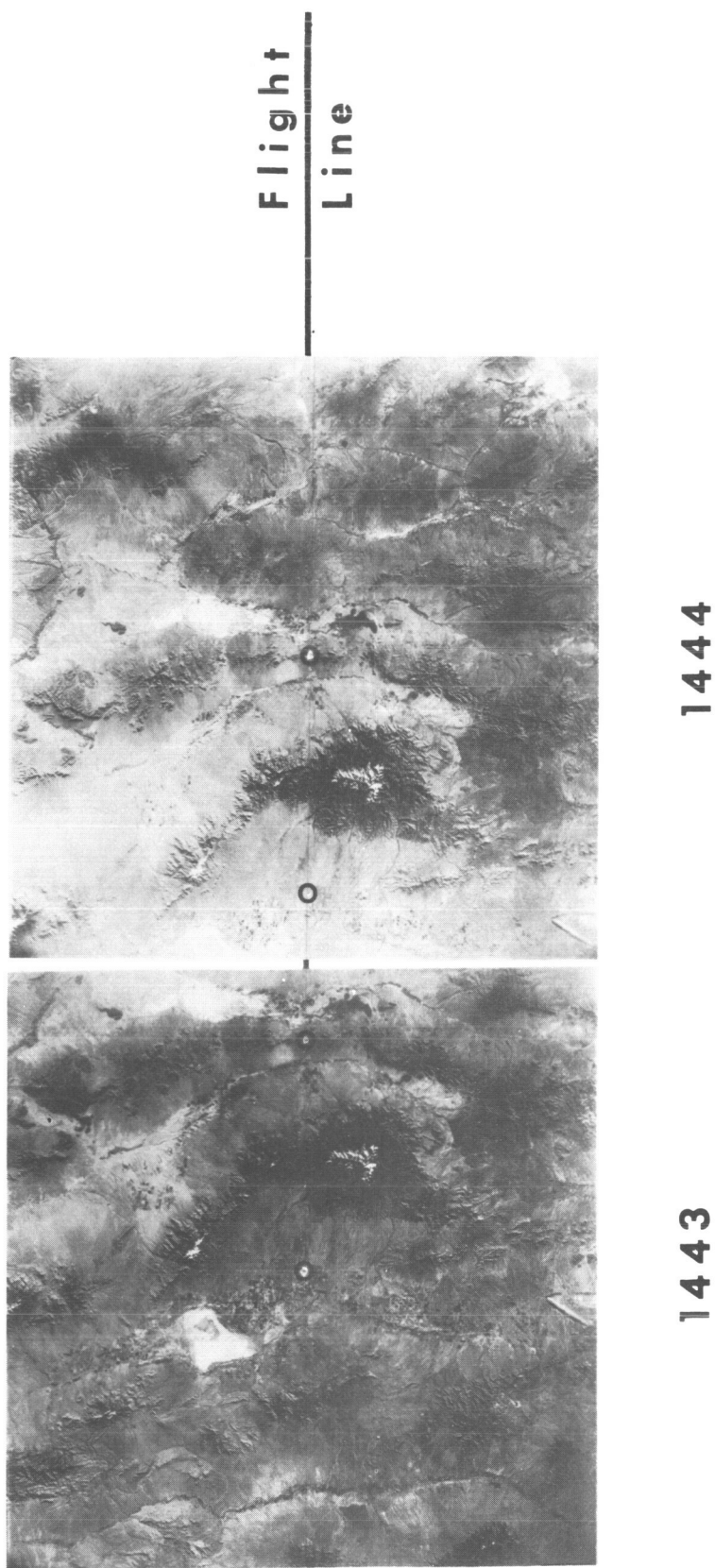


FIG. 6. STEREOGRAM OF APOLLO 6  
ORBITAL PHOTOGRAPHS 1444 AND 1445





**FIG. 7. STEREOGRAM OF APOLLO 6  
ORBITAL PHOTOGRAPHS 1443 AND 1444**

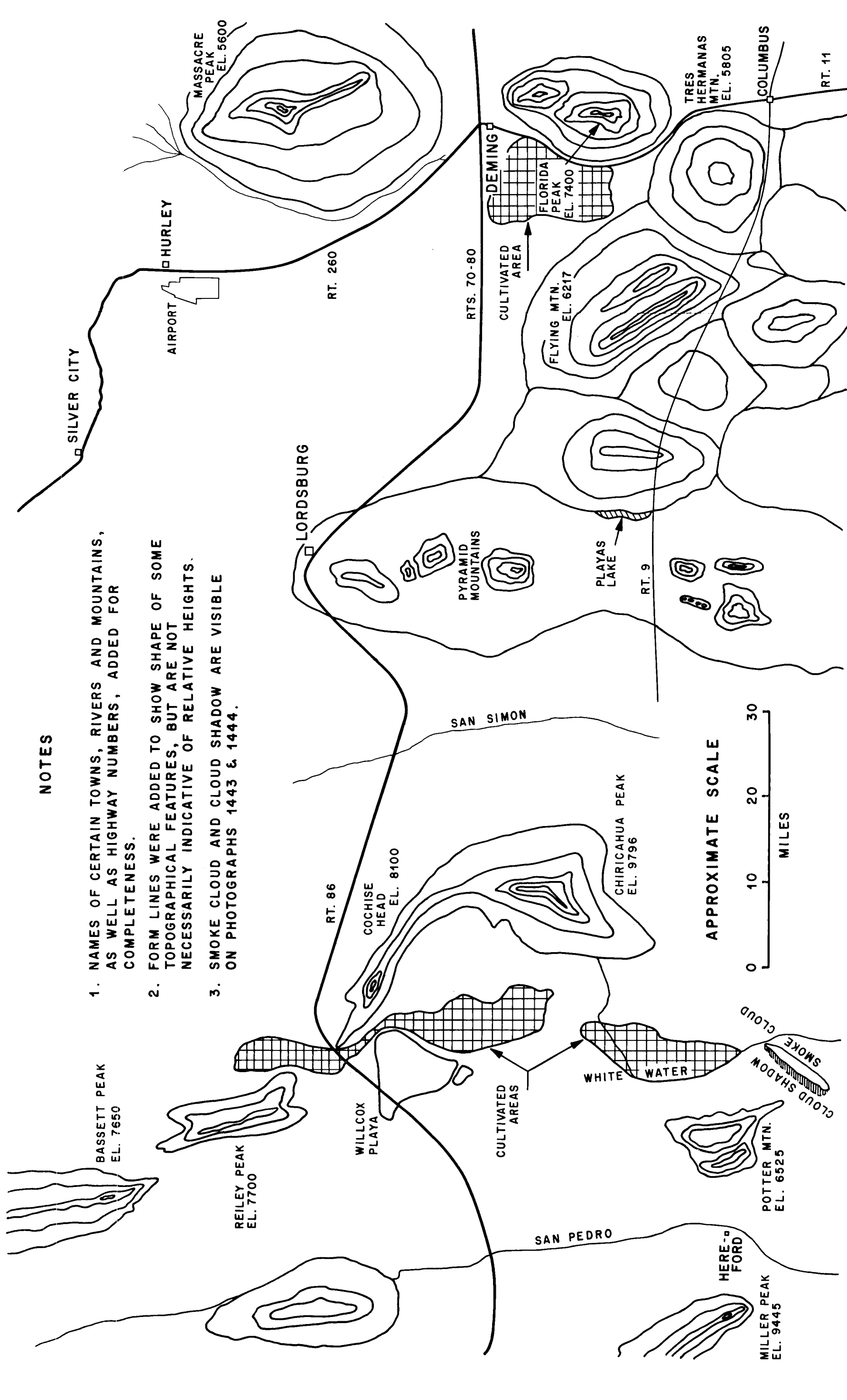


FIG. 8. TOPOGRAPHIC INFORMATION INFERRED FROM APOLLO 6 PHOTOGRAPHS 1443, 1444, AND 1445

Names of some of the larger highways, playas, mountains, rivers, and towns were added to the map to make it more complete. Topographical analyses and photogrammetric measurements of certain physical features revealed on the photographs are shown on pages 21 through 24.

In actual practice, maps such as figure 8 are not usually plotted by hand, but are prepared by using stereoprojection plotters, of which there are many types. These plotters employ the basic principle of projecting two overlapping photographs onto a plotting table where they are viewed stereoscopically, and the resulting contours are delineated on the drawing by an operator. This hand sketch was included to illustrate the ease with which a topographic map of an area can be prepared using orbital photography. Furthermore, orbital photography resulting from Skylab, together with existing topographic maps, should play an important role in earth resources analyses, and perhaps urban analyses.

"Analyses of Gemini and Nimbus photographs have demonstrated that some features, known to be associated with mineral deposits, are visible from orbital altitudes. At least one 'low level' geothermal anomaly has been imaged from aircraft, and it may be that infrared observations from space will assist in our search for sources of geothermal power. Many petroleum deposits are localized by structural features such as folds or faults. It is likely that many as yet unknown structural features will be more easily recognizable on photographs produced from orbit than on photographs produced from aircraft. Orbital photographs can include large areas in a single exposure with uniform shadows and illumination. Many metallic mineral deposits are near or along faults, and the use of aerial photographs for mapping faults and other linear features has been demonstrated. Color photography has also been a useful tool in mineral exploration, and this has led to the discovery of many mineral deposits" (quoted from reference 5).

1. Photographic Interpretations from a Stereogram Prepared from Apollo 6 Photographs 1444 and 1445

The stereographic pair composed of frames 1444 and 1445, from which certain elevation differential measurements were made photogrammetrically, is shown in figure 6. The right-hand member of this pair was shown previously at a larger photographic scale as figure 5, to assist the reader in identifying certain geographical and topographical features, if a stereoscope is not available to him. When viewing the pair 1444/1445 through a stereoscope, the most prominent features near the center of the stereogram are the Pyramid Mountains, the northernmost portions of which contain several copper, gold, silver, lead, zinc, and perlite mines. These mountains are bounded to the north by Lordsburg Draw and U. S. 80, a four-lane dual highway, which curves around the end of the Pyramid Mountain Range. Just to the west of the northern portion

of the Pyramid Mountains, one can observe a large white area, which is composed of one relatively large and two smaller alkali flats, or playas. The relatively dark areas in the playas are more moist than the lighter areas. Immediately to the west of the southern portion of the Pyramid Mountains lies a valley containing fields in cultivation. The Animas Mountains are visible south of the Pyramid Mountains, and are bordered by the Animas Valley to the west, and the Playas Valley to the east. The dark boot-shaped area on the west side of Animas Valley is a heavily forested area. Immediately to the west of Animas Valley is the Peloncillo Mountain Range which extends from top to bottom on the west side of this stereo pair. The arrowhead-shaped landform to the east of center, is bordered on the west by Playas Lake and on the east by Hachita Valley. The mountains in the center of this landform are known as the Little Hatchet Mountains. The large playa in the lower right-hand corner of the stereogram is inside the Mexican border. To the north of the Pyramid Mountains (center of stereogram), beyond Lordsburg Draw and Lordsburg Mesa, one can observe the bottom slopes of a large mountainous area, which is topped by the Gila National Forest. Numerous canyons are evident at the bottom perimeter of this structure, and the Gila River is seen trending in an east-northeasterly direction around the east side of the structure. The very sharp ridged "Black Mountain" located at the center of the base of the above described structure, and adjacent to the Gila River, marks the location of a manganese mine. The dark, heavily forested area east of the Gila River is the Gila National Forest on top of the Big Burro Mountains. Numerous copper, gold, silver, and manganese mines are located in the Big Burro Mountains area.

Highway 80, in approximately the mid-section of the stereogram, is visible from a town named Wilna, in the east, to San Simon, in the San Simon River Valley, west of the Peloncillo Mountains.

## 2. Photogrammetric Measurements from Apollo 6 Photographs 1444 and 1445

On the stereogram made from Apollo 6 Photographs 1444 and 1445, shown as figure 6, elevation differences were photogrammetrically measured between Hachita Peak and Playas Lake (points A and B on figure 5), and between Hachita Peak and the northeast corner of South Alkali Flat (point C on figure 5). For the photographs 1444 and 1445, the average orbital height  $H'$  was 702,749 feet, and the average photographic base  $b$  measured on the stereogram is 33.2 mm. The average differential parallax,  $\Delta p$ , based upon seven parallax measurements between Hachita Peak (A) and Playas Lake (B) was calculated to be .111 mm. Substituting these values in the equation described earlier in section III-A, yielded a  $\Delta h_{A-B}$  of 2350 feet. Referring to USGS Map number NH 12-3, entitled "Douglas," 1967 Revision [6], it was determined that the actual difference in

elevation between these two points was 2378 feet. The percent error between actual and photogrammetric measurement was then calculated to be 1.17.

Seven parallax measurements on both Hachita Peak (A) and the northeast corner of South Alkali Flat (C) yielded an average differential parallax  $\Delta p_{A-C}$  of .117 mm. This yielded a  $\Delta h_{A-C}$  of 2480 feet. Referring to the USGS map described in reference 6, as well as USGS Map NI 12-12 entitled "Silver City," revised in 1962, scale 1:250,000 [7], the actual  $\Delta h_{A-C}$  was shown to be 2528 feet. This resulted in an error of 1.9 percent between actual and photogrammetric measurement. Table IV summarizes the results of the photogrammetric measurements made from the stereogram composed of Apollo 6 Photographs 1444 and 1445, shown in figure 6.

Table IV. Results of Photogrammetric Measurements Made on Figure 6

Two Points Considered	$\Delta h$ (ft) Determined Photogrammetrically	$\Delta h$ (ft) Determined from USGS Map	Percent Error
A,B	2350	2378	1.17
A,C	2480	2528	1.9

### 3. Photographic Interpretations from a Stereogram

Prepared from Apollo 6 Photographs 1443 and 1444

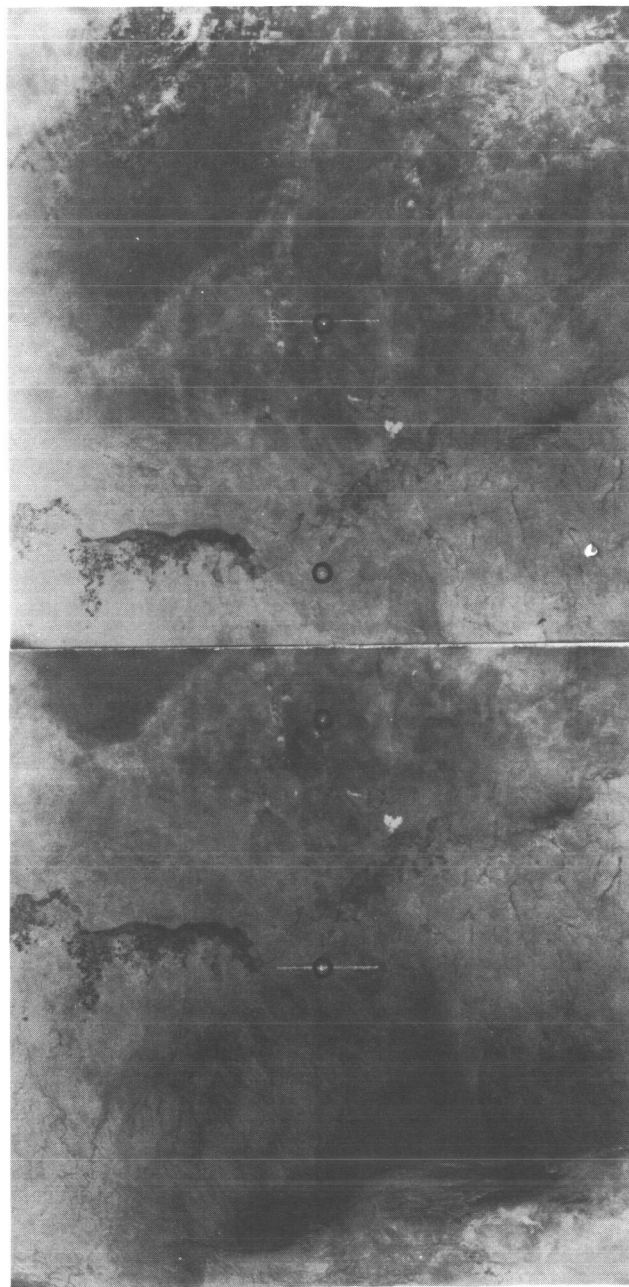
The stereographic pair, composed of frames 1443 and 1444, is shown as figure 7. The left-hand member of this stereogram is shown at a larger scale in figure 3, to assist the reader in identifying certain features discussed below, if a stereoscope is unavailable. This stereogram is bounded on the east by the three playas in the Animas Valley, discussed in connection with stereo pair 1444/1445. The Willcox Playa is visible at the western side of the stereogram. Residual moisture is evident in the eastern half of Willcox Playa. To the north of Willcox Playa, the two light lines trending northeast to southwest are the four-lane dual highway 86 (the northernmost line), and the Southern Pacific Railroad (the southernmost line). The railroad cuts across the northwestern lobe of Willcox Playa. Both the highway and the railroad diverge from Willcox (population approximately 2,500), a town about four miles north of the playa. The Chiricahua Mountains are very prominent in the stereogram center, with their heavily forested slopes, and snow-capped peaks. The Coronado National Forest encompasses

the entire area of the Chiricahua Mountains, and the extreme southern portion of the Peloncillo Mountains, visible in the southeastern quadrant of the stereogram. North of the Chiricahua Mountains, in the San Simon Valley, some areas in cultivation can be seen. To the east and south of Willcox Playa, in Sulphur Springs Valley, the land appears to be quite amenable to farming, as evidenced by the very large number of cultivated fields. In the extreme southwest corner of the stereogram, one can observe a cloud of smoke several miles long, emanating from one of the copper smelter chimneys to the east of Douglas, Arizona. In the northeast quadrant of the stereogram, in the center of the Peloncillo Mountain Range, just to the west of the northernmost playa in the Animas Valley, is a star-shaped set of small mountains. To the west, northwest, and southeast of this structure, there are several small structures which appear to be extinct volcano craters.

#### C. Earth Resources Observations and Photogrammetric Measurements from Apollo 6 Photographs 1451 and 1452

The locations of the principal points of Apollo 6 photograph frames 1451 and 1452 are  $32^{\circ}26'N$  latitude,  $104^{\circ}23'W$  longitude, and  $32^{\circ}29'N$  latitude,  $103^{\circ}44'W$  longitude, respectively. The area photographed, then, lies in the physiographic region known as the "Great Plains Region," which includes part of west Texas, eastern New Mexico, eastern Colorado, the Oklahoma panhandle, western Kansas, almost all of Nebraska, western North and South Dakota, northeastern Wyoming, and eastern Montana. The Great Plains Region is characterized by broad river plains and low plateaus on weak stratified sedimentary rocks. This area rises toward the Rocky Mountains at some locations to over 6,000 feet.

The stereographic pair, composed of frames 1451 and 1452, is shown in figure 9. The left-hand member of this stereo pair is shown at a larger photographic scale on figure 10 to assist in identifying certain geographical and topographical features, if a stereoscope is not available. Stereographic coverage is provided by this pair, for an area extending from about 15 miles west of Lake McMillan, New Mexico, to a point about 36 miles east of the city of Carlsbad, New Mexico. The north and south boundaries of this stereogram are about 50 miles from Carlsbad, New Mexico. The path of the Pecos River can be seen from the northwest corner of the stereogram to the southeast corner. In the lower part of the northwest quadrant, Lake McMillan is quite prominent at the southern end of a 30-mile-long area of crops in cultivation along the western side of the Pecos River. The marsh or swampy area north of Lake McMillan contains a large number of oil wells, and some farms and ranches are located on the land adjacent to this marsh area. To the east of the marshland area, there are numerous dendritic drainage patterns flowing toward the



Flight  
Line

1452

1451

FIG. 9. STEREOGRAM OF APOLLO 6  
ORBITAL PHOTOGRAPHS 1451 AND 1452





FIG. 10. APOLLO 6

ORBITAL  
PHOTOGRAPH

1451



Pecos River Bed. In the approximate center of the stereogram is an alkali flat or playa called Salt Lake which lies 5 miles east of Loving, New Mexico. This dry lake (elevation 2,900 feet) was one of the stations used when elevations were measured photogrammetrically on this stereogram. Just below the left center of the stereogram, a 700-foot bluff overlooking the Black River Valley can be seen. The white wavy line along the ridge of this bluff is Route 7, leading from Whites City, New Mexico, on Routes 180/62, out to the Carlsbad Caverns National Park Administration Building. The left-hand member of this stereo pair (refer to figure 10) shows the Guadalupe Ridge extending to the southwest from the Carlsbad Caverns area. North of this ridge are the Guadalupe Mountains. Several canyons, visible on the south side of Guadalupe Ridge, drain into the Black River bed. North-northwest of the Carlsbad Caverns area is the Azotea Mesa where many ranches are located. The dark, heavily forested area trending generally northward from the Guadalupe Mountains is the Lincoln National Forest.

Photogrammetric Measurements from a Stereogram Prepared  
From Apollo 6 Photographs 1451 and 1452

On the stereogram prepared from Apollo 6 photographs 1451 and 1452 (figure 9) elevation differences were photogrammetrically measured between a point half way between Whites City and the Carlsbad Caverns Administration Building (Point A, figure 10), and a point in the northeast corner of a salt lake, 6 miles east of Loving (point B). Elevation differences were also photogrammetrically determined between Point B and a point at the south side of the overpass of Route 180 over the Black River (Point C). For photographs 1451 and 1452, the average orbital height  $H'$  was 694,000 feet, and the average photographic base  $b$  measured on the stereogram was 33.35 mm. The average differential parallax,  $\Delta p$ , based upon seven parallax measurements made on both point A and point B was calculated to be .0657 mm. Substituting these values in the equation described in section III-A, yielded a  $\Delta h_{A-B}$  of 1365 feet. Referring to the USGS Map number NI 13-11 entitled "Carlsbad," 1962 Revision, Scale 1:250,000 [8], it was determined that the actual difference in elevation between these two points was 1300 feet. The percent error between actual and photogrammetric measurements was then calculated to be 4.76.

The average differential parallax,  $\Delta p$ , based upon seven parallax measurements made on both points B and C was calculated to be  $\Delta p_{B-C} = .0314$  mm. Substituting this value, and the values for  $H'$  and  $b$  previously mentioned for the case of points A and B, into the equation used for calculating  $\Delta h$ , yielded a  $\Delta h_{C-B}$  of 653 feet. USGS Map Number NI 13-11 [8] provided a  $\Delta h_{C-B}$  of 600 feet. The percent error between actual and photogrammetric measurement was then calculated to be 8.1. Table V summarizes the results of the photogrammetric measurements made from the stereogram composed of Apollo 6 Photographs 1451 and 1452 (figure 9).

Table V. Results of Photogrammetric Measurements Made on Figure 9

Two Points Considered	$\Delta h$ (ft) Determined Photogrammetrically	$\Delta h$ (ft) Determined from USGS Map	Percent Error
A,B	1365	1300	4.76
C,B	653	600	8.1

D. Photogrammetric Measurements and Photographic Interpretations  
from Apollo 8 Lunar Orbital Photographs 2066 and 2067

Apollo 8 photographs 2066 and 2067 are part of the planned lunar photography that was successfully accomplished by astronauts Frank Borman, James Lovell, and William Anders. Apollo 8 was launched from Cape Kennedy, Florida, on December 21, 1968, completed 10 lunar revolutions, and returned to earth on December 27, 1968.

The stereogram constructed from photographs 2066 and 2067 is shown in figure 11. Photograph 2066 at a larger scale is shown as figure 12 to help the viewer who does not have a stereoscope at his disposal. When these Apollo 8 lunar photographs were being studied, use was made of Lunar Planning Chart (LOC-4), Scale 1:2,500,00, Edition 1, July 1969 [9], to help determine the correct photograph orientations.

Geographical coordinates of the principal points of these photographs are shown in Table VI.

Table VI. Geographical Coordinates of Principal Points  
of Apollo 8 Photographs 2066 and 2067

	2066	2067
Latitude	-7°43' 55.689"	-7°56' 15.795"
Longitude	-169°12' 28.145"	-170°09' 36.764"

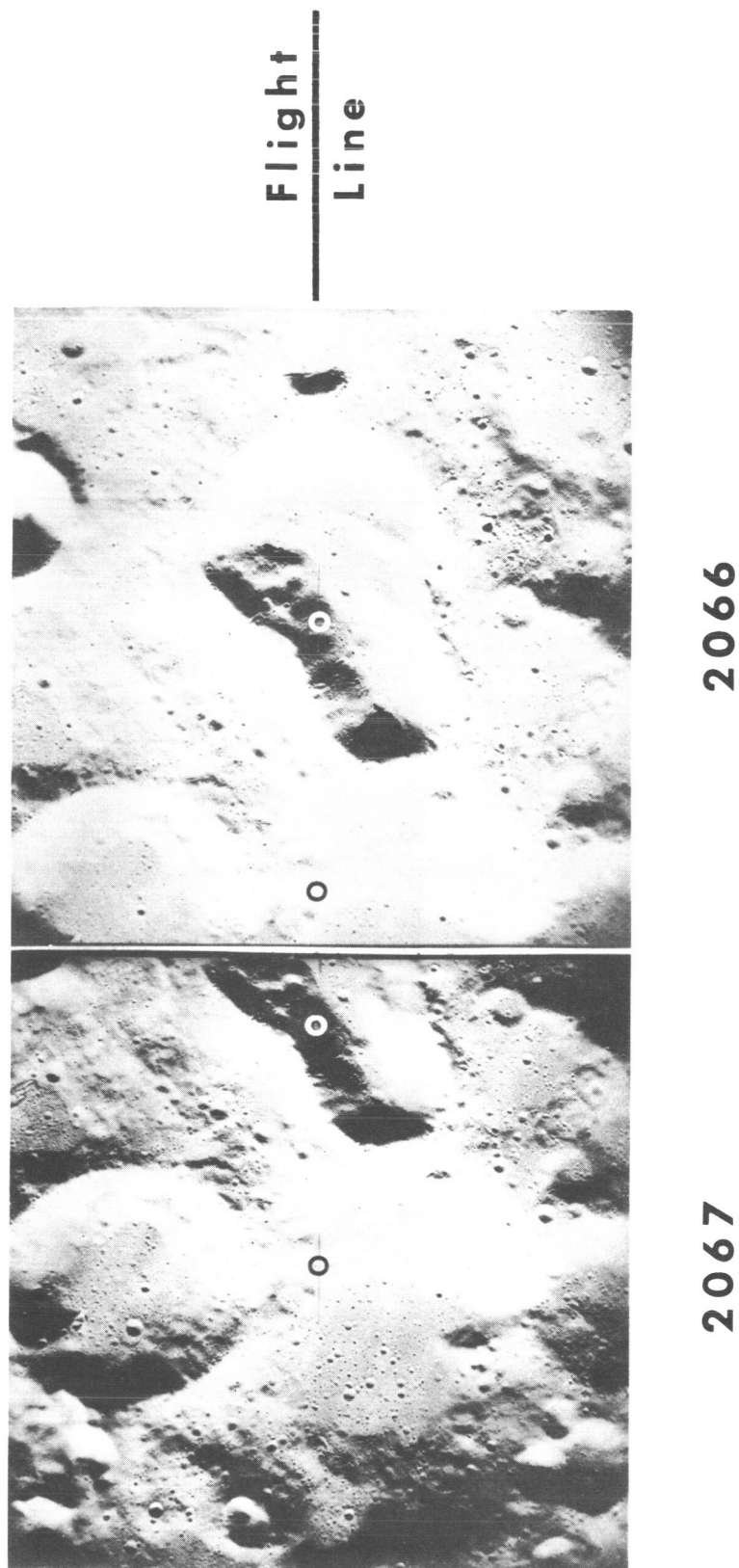


FIG. 11. STEREOGRAM OF APOLLO 8  
LUNAR ORBITAL PHOTOGRAPHS 2066 AND 2067



**FIG. 12. APOLLO 8  
LUNAR ORBITAL PHOTOGRAPH 2066**

The altitudes of the camera stations above the lunar surface for photographs 2066 and 2067 were 112,131.9 meters and 112,130.7 meters, respectively. The location pictured is to the west of Craters Korolev, Krylov, and Doppler, and to the author's knowledge, the craters in the photograph are unnamed. The oblong-shaped crater in the center of the stereogram appears to be quite deep and to contain many smaller craters. The smooth (eroded) rim indicates that the crater is relatively old.

Photogrammetric measurements of elevation differences between various points on the stereogram are discussed below. Actual points, for which elevation differences were measured, are marked on the enlarged photograph (figure 12).

"The exposures for the stereo strips taken during the Apollo 8 mission, were made every 20 seconds, using an intervalometer. Each exposure overlaps the previous exposure by approximately 60 percent. This permits viewing surface points from at least two positions separated by approximately 30 km along the orbit. An orbital altitude of  $\approx 110$  km resulted in a base-to-height ratio of 0.27 which is acceptable for stereo viewing," (quoted from reference 10).

Photogrammetric Measurements from a Stereogram Prepared  
from Apollo 8 Photographs 2066 and 2067

On the stereogram prepared from Apollo 8 photographs 2066 and 2067 (Figure 11), elevation differences were photogrammetrically measured between various points. On figure 12, which is photograph 2066 at a larger scale, the following points, on which parallax measurements were made, are labelled: Point C is a point on the west rim of the "oblong" crater; point D is on the floor of a small crater immediately to the north of point C; and point E is on the floor of the next crater northeast of point D.

The average height of the camera above the surface ( $H'$ ) at the instant of exposure of the two photographs was 368,000 feet. The average photographic base measured from the stereogram is 34.95 mm. The average differential parallax,  $\Delta p$ , based upon seven parallax measurements made on both points C and D, was calculated to be .0957 mm. Substituting these values in the equation used for calculating elevation differences yielded a  $\Delta h_{C-D}$  of 1010 feet. Similarly, the average differential parallax,  $\Delta p$ , based upon seven parallax measurements made on both points D and E, was calculated to be .408 mm. This resulted in an elevation difference  $\Delta h_{D-E}$  of 4300 feet.

#### IV. SKYLAB EXPERIMENT S-190: "SIX CAMERA MULTISPECTRAL PHOTOGRAPHY"

"Skylab" is the name given by NASA to its experimental space station program designed to increase our knowledge of manned earth orbital operations and to accomplish carefully selected scientific, technological and medical investigations. The four objectives of Skylab are (1) scientific investigations in earth orbit; (2) applications in earth orbit; (3) long-duration space flights of men and systems; and (4) effective and economical development of future space programs.

Application experiments (objective number two) include development and evaluation of efficient techniques using man for sensor operation, discrimination, data selection and evaluation, manned control, maintenance and repair, assembly and setup, and mobility involved in various operations. These experiments include studies in meteorology, earth resources, and communications.

Skylab Experiment S-190, entitled "Six Camera Multispectral Photography" is one of the earth resources experiments. The objective of this Multispectral Photographic Facility is to obtain precision multispectral photography which will provide the basis for a wide range of user-oriented studies, and thereby provide an opportunity to determine the extent to which precision and repetitive multispectral photography from space can be effectively applied to the earth resources disciplines [11].

Since the beginning of Project Mercury, photographic systems used in the manned space flight program for earth photography have evolved from simple hand-held cameras without filters through various intermediate steps to the successful performance of Experiment SO 65 on Apollo 9. Experiment SO 65, which consisted of four bracket-mounted electric Hasselblad cameras with four different film/filter combinations, provided the first opportunity to study simultaneous multispectral photography from space.

Skylab Experiment S-190, which will extend the capability for multispectral photographic study in space beyond that of SO 65, will consist of six 70 mm reconnaissance cameras, which will provide a 100-foot resolution and will permit precise registration over the entire 70 mm format; whereas, SO 65 provided a 300-foot resolution and registration on only small portions of the format, thereby losing the synoptic view that is so highly valued in space photography.

The six high-precision 70 mm cameras will have matched distortion and focal lengths. The six-inch focal length lenses will provide an approximately 80 n.m. square surface coverage from the expected 235 n.m. orbit. The system will be designed for the following wavelength/film combinations:

500 - 600 millimicrons: Panchromatic x - Black and White

600 - 700 millimicrons: Panchromatic x - Black and White

700 - 800 millimicrons: Infrared - Black and White

800 - 900 millimicrons: Infrared - Black and White

500 - 880 millimicrons: Infrared - Color

400 - 700 millimicrons: High Resolution Color.

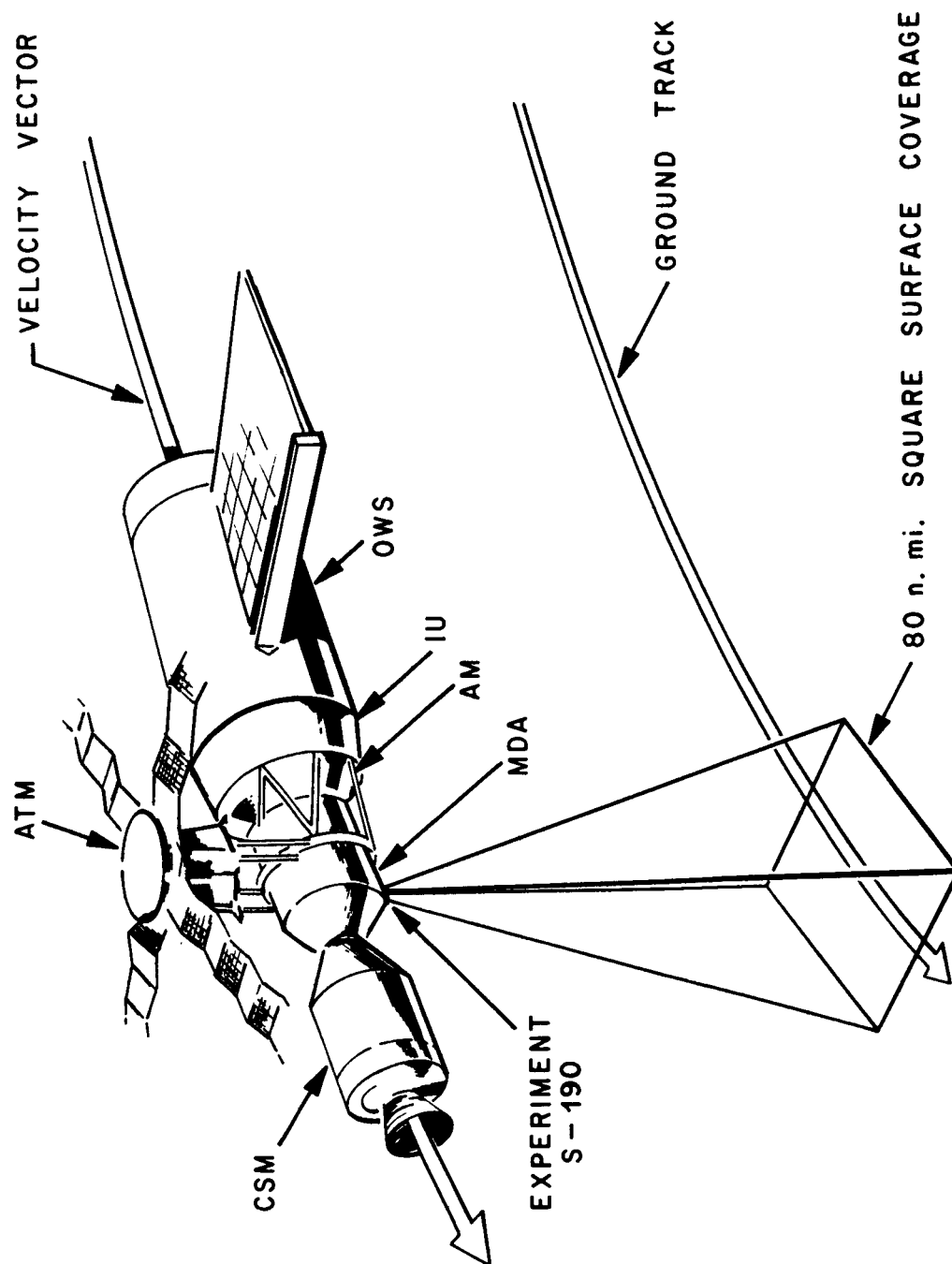
The spectral regions designated were selected to separate the visible and photographic infrared spectrum into the bands that are expected to be most useful for multispectral analysis. The selection was based on experience gained in the NASA Earth Resources Aircraft Program, the performance of experiment SO 65, and other multispectral photographic studies.

Figure 13 shows the general location of experiment S-190 in the Multiple Docking Adaptor (MDA) of Skylab, and the orientation of Skylab when experiment S-190 is being conducted.

#### V. ANALYSIS OF GROUND OBSERVABLE BY SKYLAB CAMERA THROUGH CUMULUS CLOUD COVERAGE

A brief graphical analysis was conducted to show the percentage of ground observable through varying percentages of cumulus cloud coverage, by the camera which is to be used in the Skylab. The effect of the sun's elevation, with resultant cloud shadows, was also considered. Twenty- and thirty-degree sun elevation angles (angle from horizontal to the sun's rays) were considered since these angles are specified as the minimum sun elevation angles for photography in the winter and summer hemispheres, respectively (page 18, reference 11).

The graphical analysis to this study, as shown in Figure 14, was conducted by laying out the camera station altitude of 235 nautical miles and the camera view angle of 20 degrees [12]. A perpendicular to the ground was then drawn, since the Skylab photography of the earth is planned for the vertical mode. The 20-degree camera view angle enclosed a horizontal projection or ground strip of 83 nautical miles (see figure 14). An 80-nautical-mile square surface coverage is planned for the Skylab camera S-190 Multi-Band Photography Experiment [11]. Representations of assumed cloud coverages were then constructed on the drawing, and rays were drawn from the camera's perspective center to the ground,



**FIG. 13. LOCATION OF SKYLAB EXPERIMENT S-190**



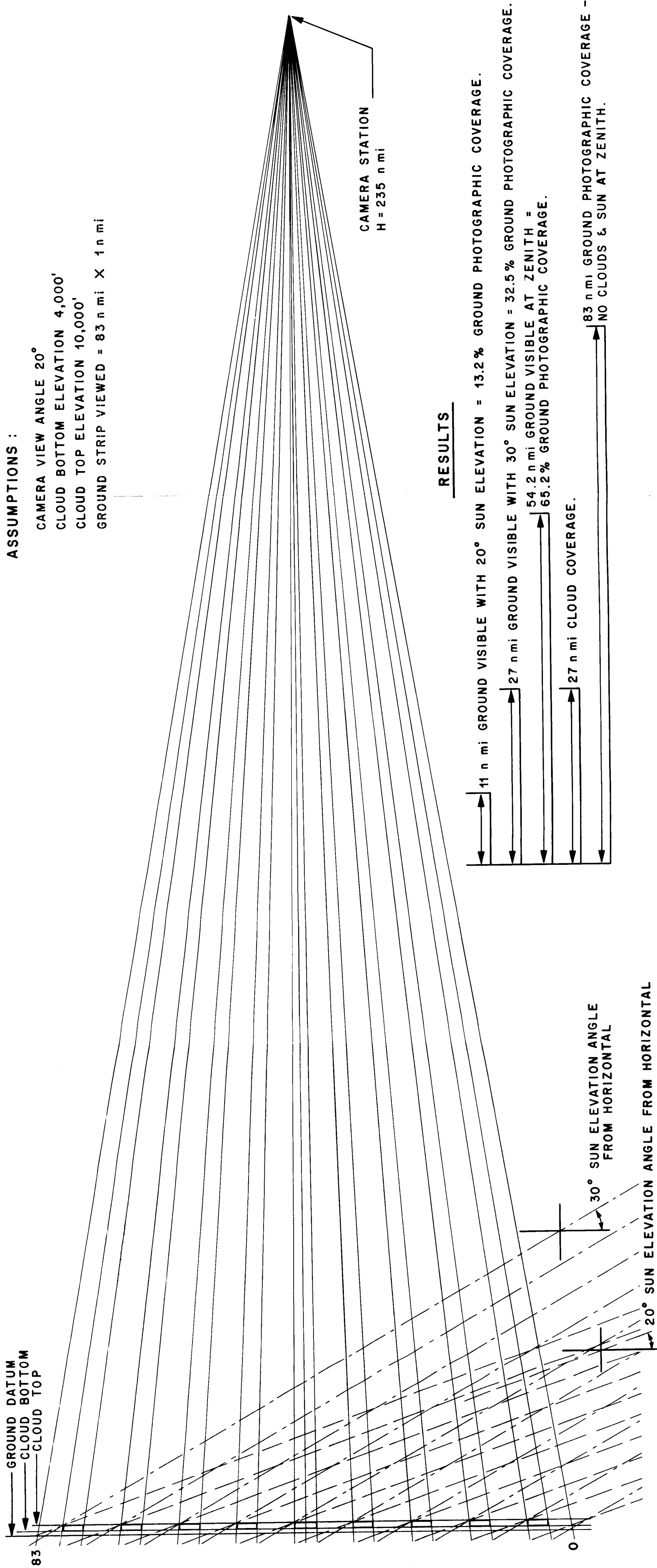


FIG. 14. GROUND OBSERVABLE BY SKYLAB CAMERA THROUGH 32.5 % CUMULUS CLOUD COVERAGE

and tangent to the sides of each cloud. Intersections of the tangents with the ground datum were constructed. The sum of the pieces of the ground strip which could then be observed by the camera (i.e., those which were not covered by clouds) was noted, and this value divided by the total strip length was considered to be the percentage of ground observable at zenith (sun elevation  $90^\circ$ ).

For the case of determining the ground observable at sun elevations other than zenith, sun rays were drawn (figure 14) at the appropriate angle to the ground, and tangent to the cloud representations. Intersections of these rays with the ground datum were noted, and measurements were made of the strip which was observed in the "zenith" case minus the loss due to the shadow formed by the sun at the assumed elevation. The sum of these difference elements was divided by the total strip length to obtain the percentage of ground observable, taking into account the shadows due to the sun. Figures 15 and 16 summarize the results of this analysis (1) by showing the percentage of ground observable versus sun angle or elevation, assuming a 32.5 percent cumulus cloud cover, and (2) by showing the percentage of ground observable versus the percentage of cumulus cloud cover, assuming a 20-degree sun elevation.

## VI. SEVERAL RECENT PHOTOGRAMMETRIC APPLICATIONS BY UNIVERSITIES, COMPANIES, AND OTHER GOVERNMENT AGENCIES

As mentioned in section II of this report, the applications of photogrammetric techniques to activities associated with earth resources and earth problems are many and varied. Included in this section are brief descriptions of four interesting recent applications of photogrammetry to various problems, namely, the mapping of earth's terrain, the mapping of polluted air masses, the determination of thermal pollution in bodies of water, and the gathering of geoscientific data in areas notorious for persistent cloud coverage, by using side-looking airborne radar.

### A. Side Looking Airborne Radar (SLAR) as a Geophysical Tool

Side-looking airborne radar (SLAR) is a versatile remote-sensing tool, in that it can be used during the day or night, under many weather conditions. It provides large area coverage and high data acquisition rates. The disadvantages of SLAR compared to conventional aerial photography are (1) poorer image resolution, (2) susceptibility to electronic noise, and (3) complexity of equipment. Figure 17 shows a radar mosaic of Darien Province in Panama and parts of northwest Colombia in South America, at an approximate scale of 1:250,000. This area is perpetually

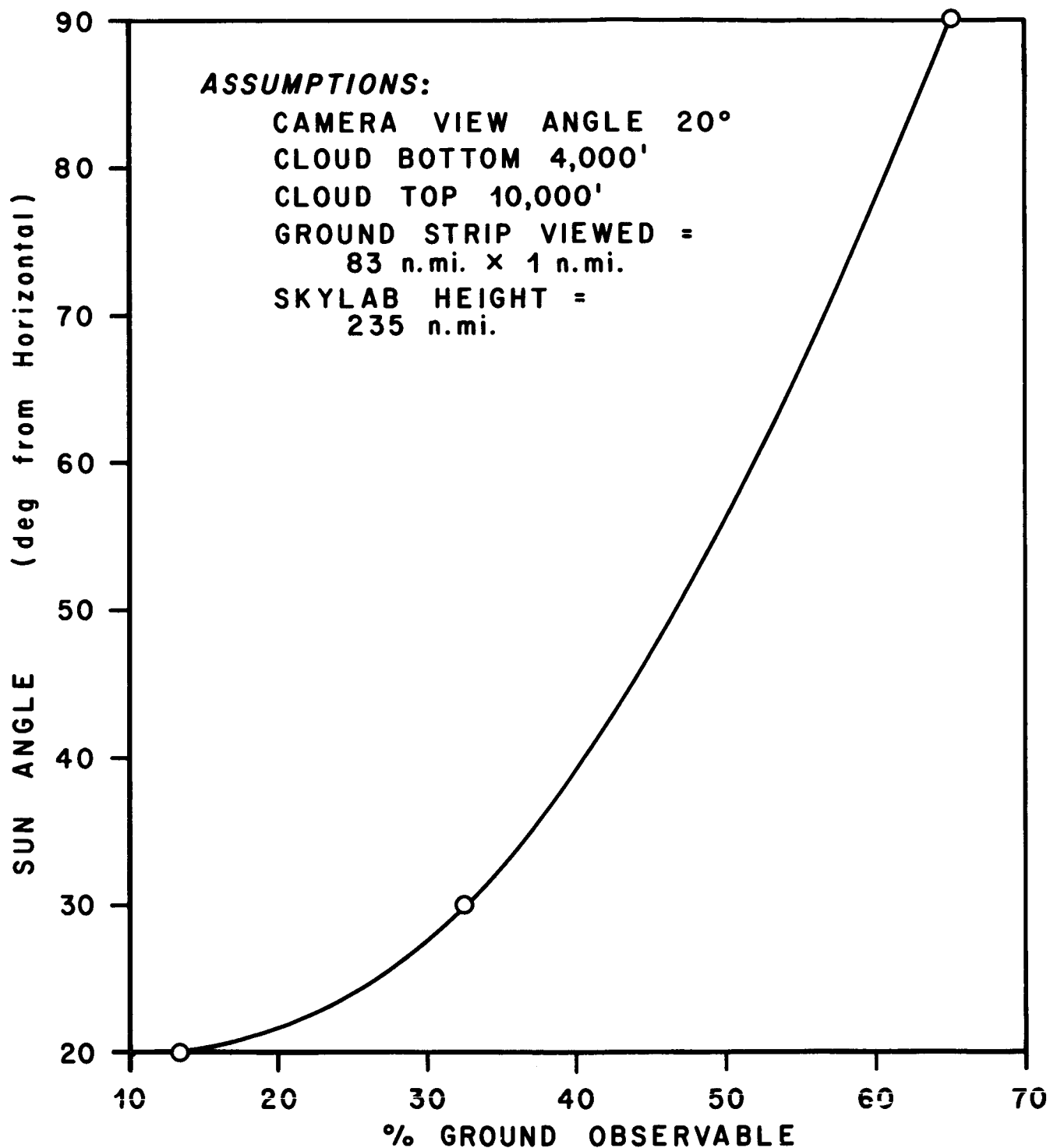


**FIG. 15. GROUND OBSERVABLE BY SKYLAB CAMERA THROUGH 32.5% CUMULUS CLOUD COVER VERSUS SUN ANGLE**

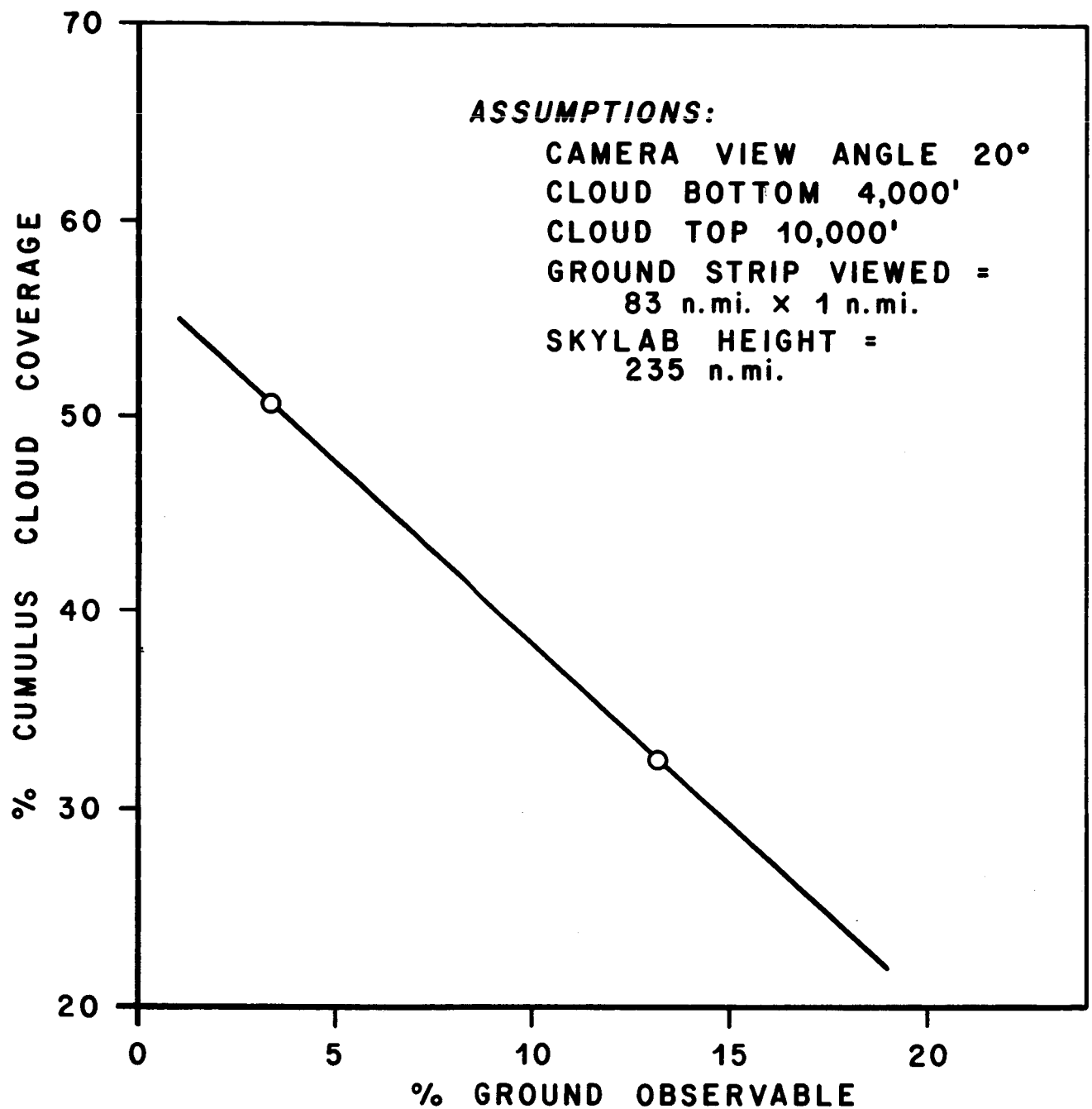


**FIG. 16. GROUND OBSERVABLE BY SKYLAB CAMERA AS A FUNCTION OF CUMULUS CLOUD COVERAGE ASSUMING A  $20^\circ$  SUN ELEVATION**

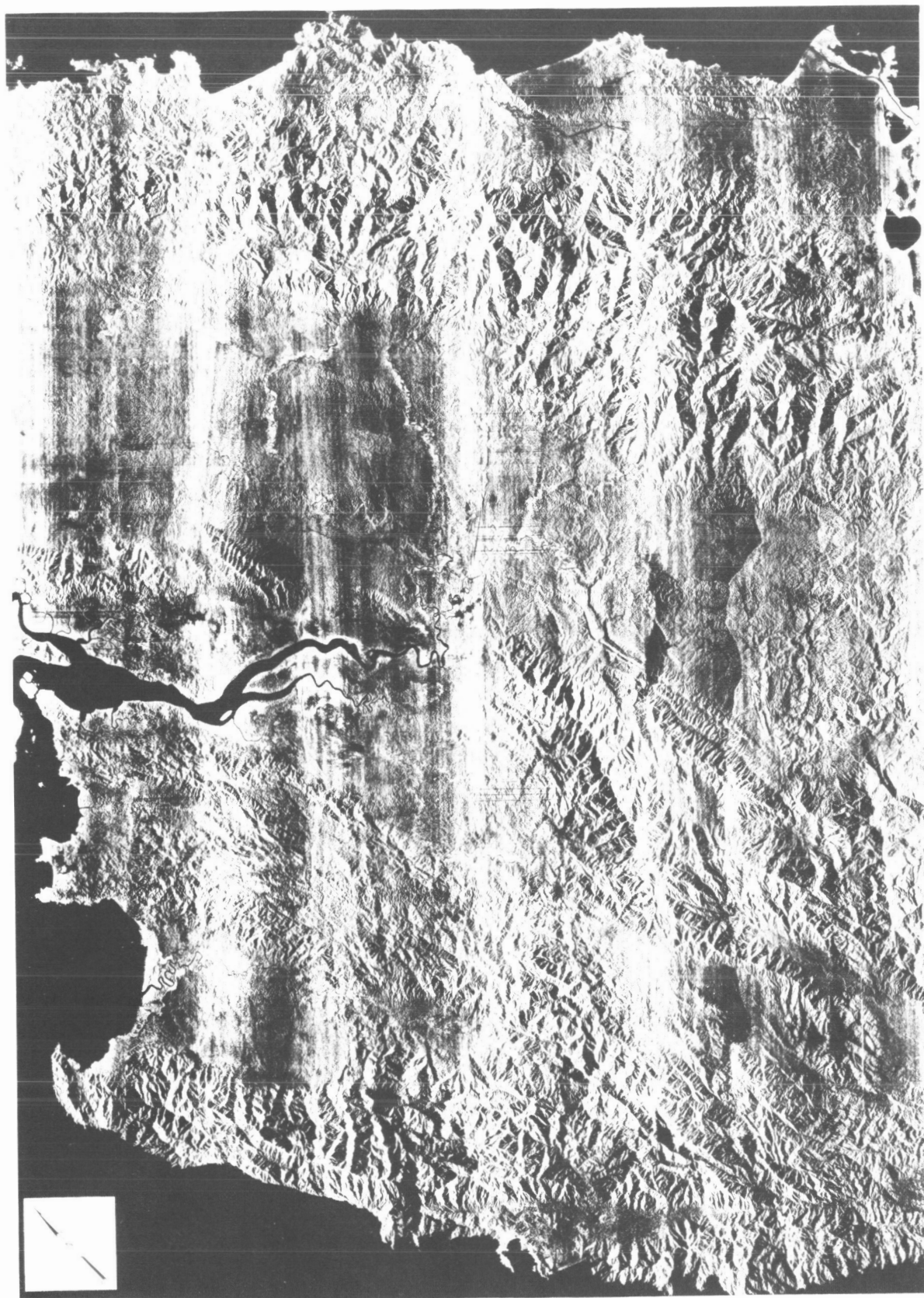


**FIG. 17. RADAR MOSAIC OF DARIEN PROVINCE, PANAMA, & NORTHWEST COLOMBIA, SOUTH AMERICA**

cloud-bound. Under a U. S. Army Corps of Engineers contract, the Westinghouse AN/APQ-97 side-looking airborne radar was used to acquire imagery of approximately 6600 square miles. This coverage was obtained within four hours of flying time. The Raytheon Company, Autometric Operation, who provided the photograph shown in figure 17, was assigned the task of preparing this semi-controlled mosaic. A series of geoscience overlays, such as surface drainage, surface configuration, vegetation, and engineering geology, which were subsequently prepared by that company, is indicative of the types of geoscientific information obtainable from SLAR imagery [13]. SLAR surveys may now be considered as supplemental geophysical tools in support of fuel and mineral exploration.

#### B. Thermal Pollution Revealed by Infrared Radiation

The image shown in Figure 18 illustrates the results of a method by which thermal pollution in a body of water can be revealed. Using infrared line-scanning techniques, the emitted radiation from the terrain was received by a detector in an aircraft at 1500 feet altitude, traveling at a ground speed of 150 miles per hour. The location shown is East Haddam Neck, Connecticut, on the Connecticut River, approximately 30 miles below Hartford. The object of the imagery was to reveal the thermal discharge from the nuclear-power generation station (north end of the river, on the east bank), and to show how it spreads into and over the surface of the Connecticut River, as well as to show how it thermally pollutes the flow of the smaller river which feeds into the Connecticut River further south of the nuclear power generation station. In this imagery, the thermally enhanced objects can be more readily seen, since they are better emitters, in relation to the detector used, for receiving the infrared signals. Infrared radiation signals received by the detector and stored by one of various methods were then converted to light signals, which were put on photographic film in such a manner as to result in the imagery shown. The detector used to receive the infrared signals was designed to receive emissions whose wavelengths were between 3.7 and 5.5 microns. This imagery was furnished by the Aerospace Systems Division of Bendix Corporation, who prepared it on their commercially developed Thermal Mapping Device.

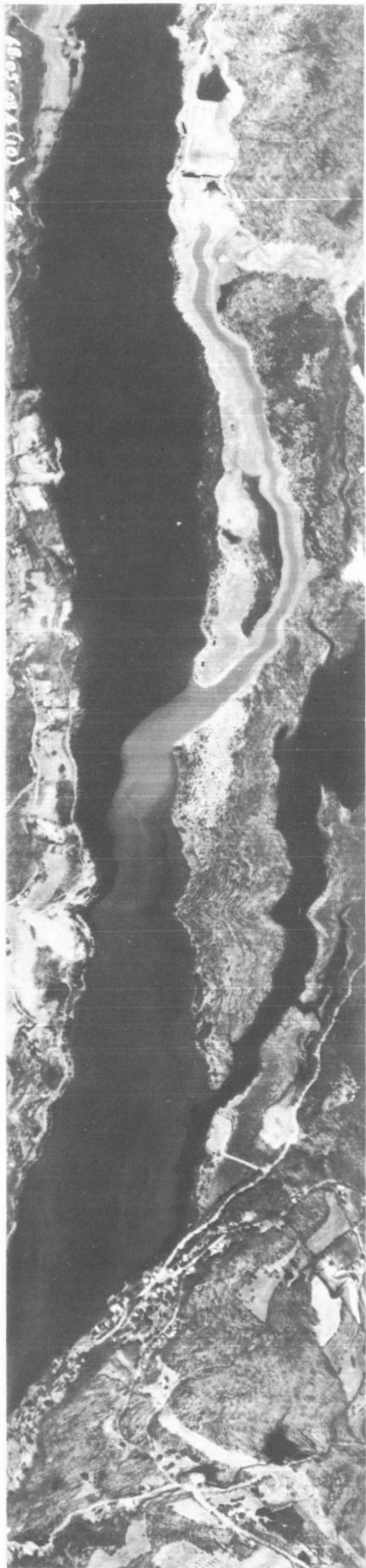


**FIG. 18.**  
**THERMAL POLLUTION**  
**IN THE**  
**CONNECTICUT RIVER**  
**REVEALED BY**  
**INFRARED RADIATION**

### C. Automatic Stereoplotting for Mapping and Measuring Polluted Air Masses

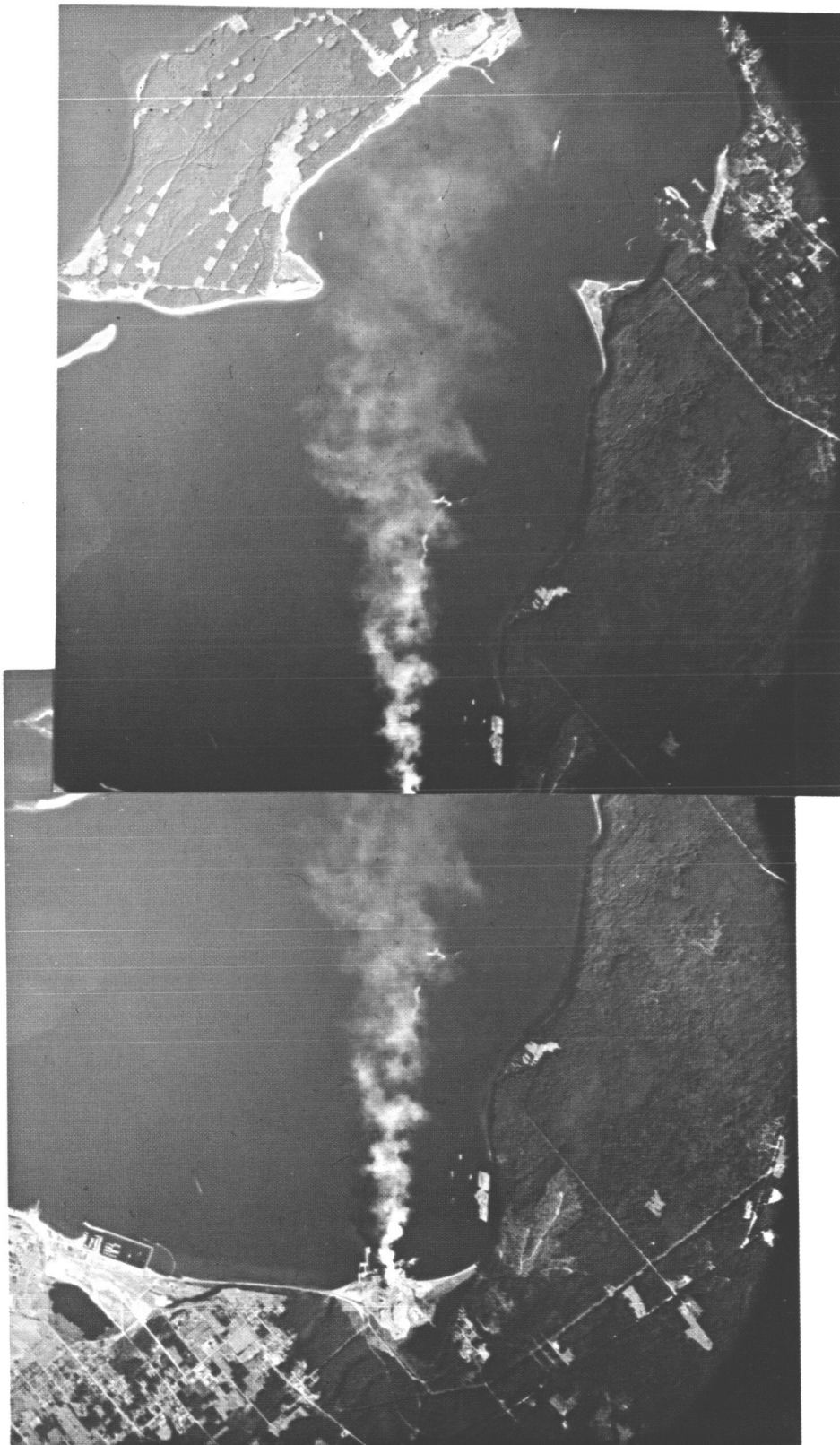
Dr. S. A. Veress, Associate Professor of Civil Engineering at the University of Washington, presented a paper at the March 1970 Annual Meeting of the American Society of Photogrammetry entitled "Determination of Concentration of Polluted Air by Photogrammetry." Dr. Veress, and his associates at the University of Washington who helped him in the conduct of this study, were supported by the National Center for Air Pollution Control, Bureau of Disease Prevention and Environmental Control, under Public Health Service Contract AP-00661-01.

Upon completion of all the work required by this contract, Dr. Veress, as principal investigator, published the final technical report, entitled "Study of the Three-Dimensional Extension of Polluted Air," [14]. The objective of the research project was to investigate the possibility of determining the photogrammetric recording of the vertical and horizontal extension of polluted air within reasonable limits of accuracy. Some of the conclusions of photogrammetric interest reported by Dr. Veress, at the completion of his study, are as follows: "The dimensions, horizontal and vertical, of the polluted air mass, can be established from aerial photographs, with satisfactory accuracy. Using vertical photographs, the horizontal accuracy is  $\pm 10$ -20 feet at the source of industrial pollution, decreasing to  $\pm 20$ -50 feet where the concentration of pollution becomes diluted to about  $500 \mu\text{gm}^{-3}$ . Using vertical photographs, the accuracy of elevation is about  $\pm 8$ -19 feet at the source, and decreases to  $\pm 100$ -150 feet at about 2 to 2 1/2 miles from the source, where the mass concentration is about  $500 \mu\text{gm}^{-3}$ . Using oblique photographs to determine the elevation of the lower and upper surfaces of the plume cone, accuracies of these elevations were found to be about  $\pm 20$  feet up to 6 miles from the source where the concentration is approximately  $150$ - $200 \mu\text{gm}^{-3}$ " (quoted in part from page 46, reference 14).

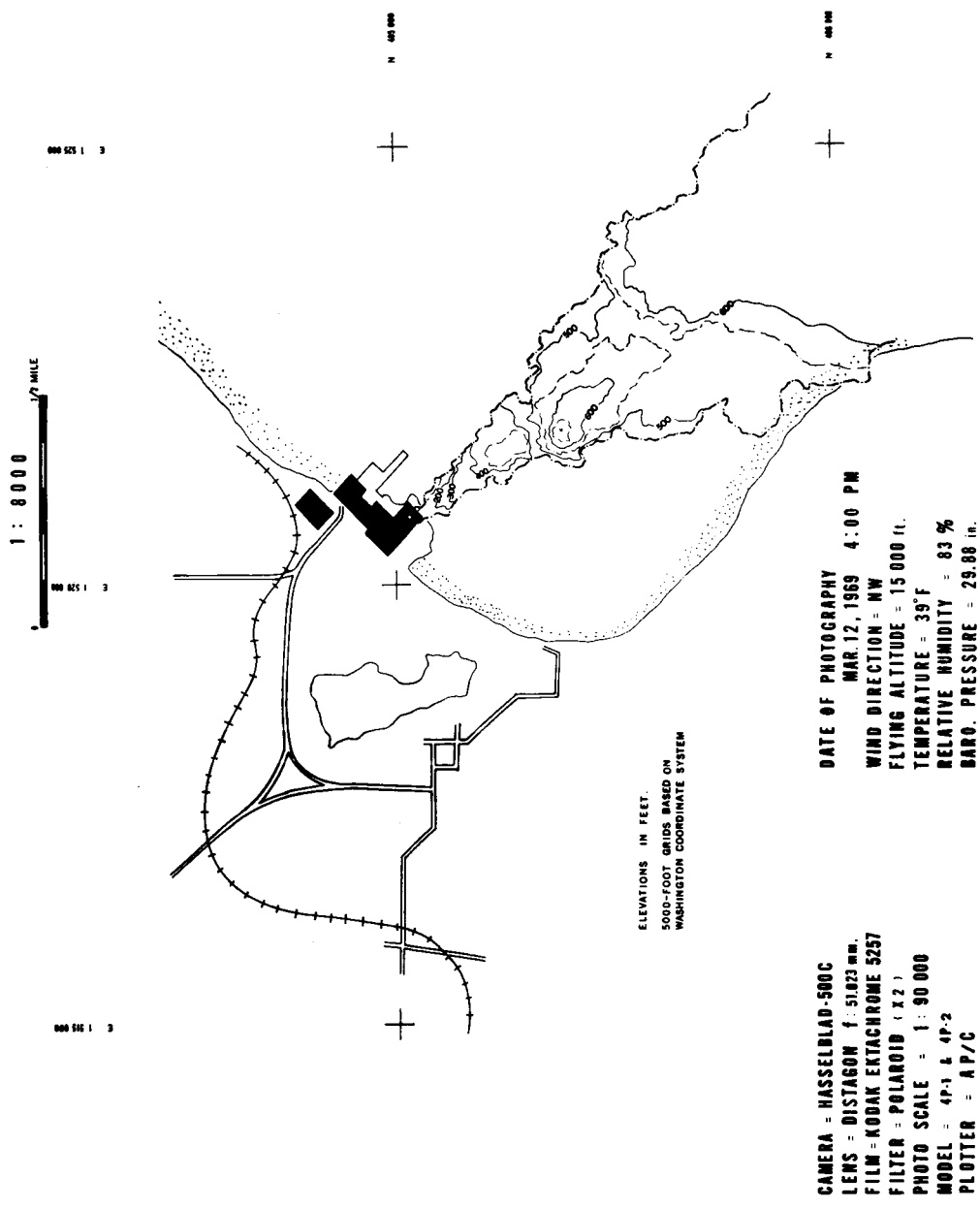
Based upon these findings, Dr. Veress concluded that "the mapping of industrial pollution using a combination of vertical and oblique photographs is possible, and that the dimensional monitoring of polluted air masses over an industrial area is feasible by photogrammetry."

Figure 19 is a stereogram prepared from vertical photographs of Port Townsend, Washington which were taken from an aircraft flying at 15,000 feet altitude. An industrial plant with a smokestack discharging smoke into the air is visible. It was from a pair of vertical photographs similar to those shown in figure 19 that a topographic map (see figure 20) of the smoke cloud, in the Port Townsend area, was made on the University of Washington's AP/C analytical plotter.





**FIG. 19. COLOR STEREOGRAM  
SHOWING AIR POLLUTION IN THE  
PORT TOWNSEND, WASHINGTON AREA**



**FIG. 20. TOPOGRAPHIC MAP OF AIR POLLUTION  
IN THE PORT TOWNSEND, WASHINGTON AREA**

#### D. "Space Age" Road Map Which Resulted from Gemini V Mission\*

An unusual by-product of space photography (a road map of Tucson, Arizona, and vicinity) has been released by the U. S. Geological Survey, Department of the Interior. This "space-age" road map, shown in figure 21, was prepared from photographs taken by Astronauts Gordon Cooper and Charles Conrad, Jr., from an altitude of approximately 100 miles, during the Gemini V mission flown during August 1965. The photomap was compiled by cartographers of the U. S. Geological Survey in cooperation with the National Aeronautics and Space Administration. To remove tilt distortions, the photograph was rectified by the Autometric Operations of Raytheon Corporation. This photograph, each side of which represents 75 miles, covers about 5500 square miles. Conventional mapping photography taken at 30,000 feet would require over 75 pictures to cover the same area.

This practical application of space photography provides a traveler with information about the Tucson area that a conventional road map or even a standard topographic map cannot provide. This map not only shows basic road information but also true land imagery. Among the features which can be discerned are the urban area, cultivated areas, mountain ranges, valleys, and large land-clearing operations, as well as linear features such as rivers and main highways. Perhaps when space imagery of this type becomes readily available, space-age road maps can be made of the entire United States, thereby adding to the enjoyment of the traveling American public.

#### VII. SUMMARY REMARKS

The scientific and engineering communities will use methods and techniques provided by the tools of photogrammetry to a greater extent in the future than they have in the past. Efficient exploitation of the earth's remaining natural resources will be aided by photogrammetric measurements and analyses of the land, sea, and air containing those resources. In like manner, man, in his search for ways and means of understanding and providing solutions for the real environmental problems that surround him today (in the areas of water and air pollution, for example), will need to depend heavily on the analytical and measurement techniques which can be provided him by photogrammetrists.

---

\* Excerpted in part from Department of the Interior News Release dated June 29, 1969, entitled: "Space-Age Road Map of Tucson, Arizona, Prepared" [15].

RECTIFIED GEMINI V PHOTOGRAPH  
TAKEN AUGUST 21, 1965 BY AS-  
TRONAUTS GORDON COOPER AND  
CHARLES CONRAD, JR.

COMPILED BY THE U.S. GEOLOG-  
ICAL SURVEY, IN COOPERATION  
WITH THE NATIONAL AERONAU-  
TICS AND SPACE ADMINISTRA-  
TION, RECTIFICATION BY RAY-  
THEON COMPANY, AUTOMETRIC  
OPERATIONS.

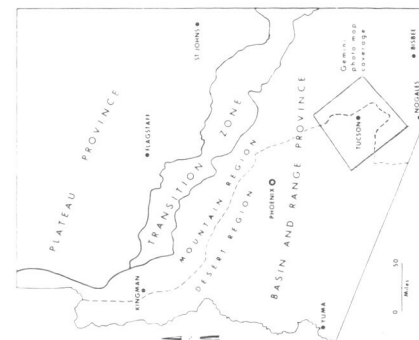
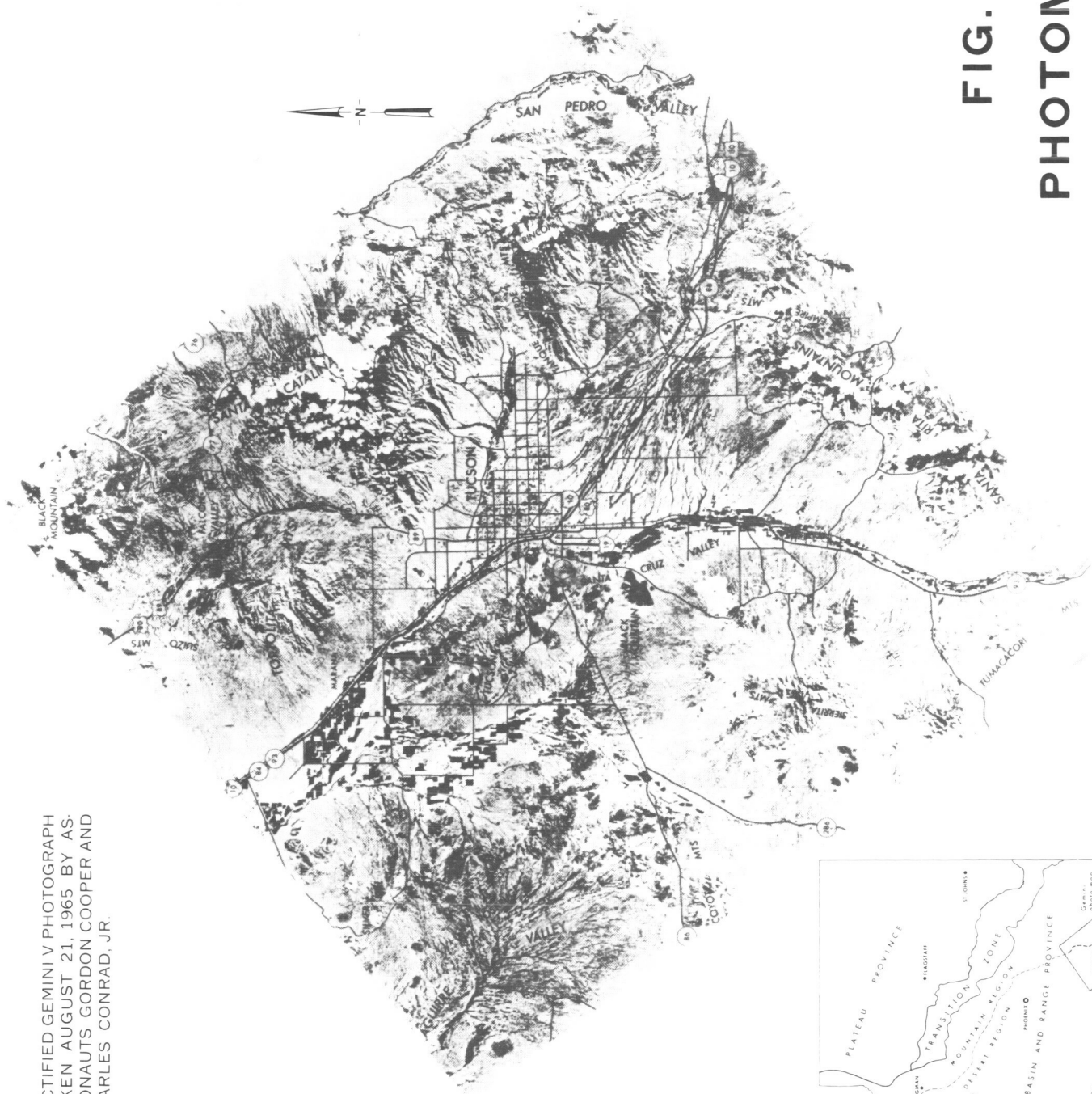
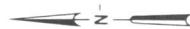


**FIG. 21. GEMINI  
PHOTOMAP OF THE  
TUCSON, ARIZONA VICINITY**

A vast and relatively untapped store of useful information for studying earth resources and problems awaits the scientist and engineer, in the form of photographic imagery of the earth, which was obtained during various flights of the Gemini and Apollo programs. Further valuable photographic information, helpful to man in studying his available resources and his environmental problems, will be secured during the Multispectral Photography experiment of NASA's Skylab in the near future, as well as in the Earth Resources Technology Satellite program in which NASA is developing experimental satellites to provide data of a type requested by the Department of the Interior.

Relatively inexpensive photogrammetric measuring instruments, together with the application of geometric principles, can be quite useful in performing photogrammetric analyses and photographic interpretations where a reasonable degree of accuracy is required. For high order, precision analytical requirements, much more exotic equipment, such as automated stereoplotters coupled with digital computers, is required.

Results of a graphical analysis indicate that, if one assumes a 32.5 percent cumulus cloud coverage and a 30-degree sun elevation angle, less than half of the ground will be visible to the Skylab cameras, within the camera's field of view, assuming that vertical photography is used.

Engineering firms which specialize in providing photogrammetric services, well qualified universities and their staffs, and experienced government agencies are available today to undertake jobs relating to photogrammetric analyses pertinent to our intelligent use of earth resources and to discover ways of solving our environmental problems by first systematically defining them by means of available photographic imagery.

## REFERENCES

1. Larsen, Paul A., "Some Photographic Results of the Apollo 11 Mission," NASA, Marshall Space Flight Center, NASA TM X-64501, February 27, 1970.
2. Army Map Service Map of Cache, Oklahoma, Sheet 6253 II, Scale 1:50,000, Orthophotoscopic Mosaic and Contours prepared by USAEGIMRADA, Ft. Belvoir, Virginia, June 1965; Pictomap prepared by Army Map Service, Corps of Engineers, U. S. Army, Washington, D. C.
3. Statement of W. T. Pecora, Director, U. S. Geological Survey, May 5, 1969, contained in NASA Authorization for Fiscal Year 1970 Hearing before the Committee on Aeronautical and Space Sciences, United States Senate, May 1, 6, and 9, 1969, Part 2, pp. 704-724.
4. Fischer, William A., "Projected Uses of Observations of the Earth from Space," The EROS Program of the Department of the Interior, U. S. Geological Survey, Washington, D. C.
5. Fisher, William A., "Satellite Detection of Natural Resources," U. S. Geological Survey, Washington, D. C., February 21, 1966.
6. United States Geological Survey Map NH 12-3, "Douglas," 1967 Revision, Scale 1:250,000.
7. United States Geological Survey Map NI 12-12, "Silver City," 1967 Revision, Scale 1:250,000.
8. United States Geological Survey Map NI 13-11, "Carlsbad," 1962 Revision, Scale 1:250,000.
9. Lunar Planning Chart (LOC-4), Scale 1:250,000, Edition 1, July 1969, prepared under the direction of Department of Defense by the Aeronautical Chart and Information Center, United States Air Force, for National Aeronautics and Space Administration.
10. Data Announcement Bulletin #NSSDC 69-06, "Apollo 8 Lunar Photography," prepared by National Space Science Data Center, Code 601, Goddard Space Flight Center, Greenbelt, Maryland 20771.
11. Experiment Implementation Plan for Manned Space Flight Experiments, "Multispectral Photographic Facility (Earth Applications)," November 24, 1969, NASA Form 1347.
12. Enclosure 10 to the Minutes of the AAP Mission Requirements Panel Meeting, February 4, 1970, "Camera Field of View."

#### REFERENCES (Continued)

13. Booklet entitled "Side-Looking Airborne Radar - A New Geophysical Tool," prepared by Autometric Operation, Raytheon Company, 4217 Wheeler Avenue, Alexandria, Virginia 22304.
14. Veress, Dr. S. A., "Study of the Three-Dimensional Extension of Polluted Air," University of Washington, Department of Civil Engineering, supported by National Center for Air Pollution Control, Bureau of Disease Prevention and Environmental Control, Public Health Service Contract AP-00661-01, May 1970.
15. Department of the Interior News Release dated June 29, 1969, "Space-Age Road Map of Tucson, Arizona, Prepared."

APPROVAL

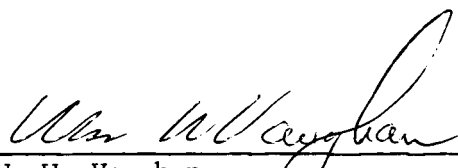
NASA TM X-64546

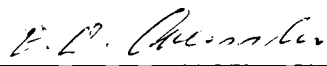
PHOTOGRAMMETRIC TECHNIQUES APPLICABLE TO EARTH RESOURCES ANALYSES

by Paul A. Larsen

The information in this report has been reviewed for security classification. Review of any information concerning Department of Defense or Atomic Energy Commission programs has been made by the MSFC Security Classification Officer. This report, in its entirety, has been determined to be unclassified.

This document has also been reviewed and approved for technical accuracy.

  
\_\_\_\_\_  
W. W. Vaughan  
Chief, Aerospace Environment Division

  
\_\_\_\_\_  
E. D. Geissler  
Director, Aero-Astrodynamics Laboratory